Accepted at *Quantitative Economics*

Three reasons to price carbon under uncertainty: Accuracy of simple rules

TON VAN DEN BREMER
Faculty of Economics and Business, University of Amsterdam, Netherlands and Faculty of Civil Engineering and Geosciences, Delft University of Technology, Netherlands

CHRISTOPH HAMBEL
Department of Econometrics and Operations Research, Tilburg University, Netherlands and Netspar

FREDERICK VAN DER PLOEG
Department of Economics, University of Oxford, United Kingdom, Faculty of Economics and Business, University of Amsterdam, Netherlands, CEPR, and CESifo

An easy-to-interpret rule for the optimal risk-adjusted social cost of carbon is derived using perturbation analysis. This rule internalises the adverse effects of global warming on the risk of recurring climate-related disasters, the risk of irreversible cascading climate tipping points, and the usual effect on total factor productivity. It and its three components approximate the true numerical optimum well, especially if the small parameters (i.e., the share of damages in GDP, the sensitivity of the risk of disasters to temperature and the risk of climate tipping) are small enough and the discount rate is not too small. The rule is also accurate if applied to AK models with a different supply side, e.g., with ongoing technical progress in fossil-fuel production or multiple economic sectors. With a growth-adjusted discount rate of 2%/year, the SCC is \$172/CO_2, 70% of which is due to recurring climate disasters and 9% to climate tipping risk.

KEYWORDS. carbon pricing, damages, recurring macroeconomic and climate-related disasters, gradual climate tipping point, perturbation analysis.

JEL CLASSIFICATION. H21, Q51, Q54.

Ton van den Bremer: t.s.vandenbremer@uva.nl
Christoph Hambel: c.hambel@tilburguniversity.edu
Frederick van der Ploeg: rick.vanderploeg@economics.ox.ac.uk
We are grateful to four anonymous reviewers for their constructive and helpful comments. We thank Fred Espen Benth, Carina Fleischer, Reyer Gerlach, Marten Hillebrand, Frank de Jong, Matthias Kalkuhl, Christos Karydas, Rüdiger Kiesel, Kai Lessmann, Armon Rezai, Christian Traeger, Sjak Smulders, Cees Withagen, Michael Wulfsohn and participants of the ASMF Seminar at the University of Amsterdam, the DEF Research Seminar at LUISS University, the Economics Workshop at Tilburg University, the PECF Research Seminar at the MCC Berlin, the QFAS Seminar at Tilburg University, the 2nd Workshop on Energy, Climate, and ESG at the University of Oslo, DEAERE 2024 conference, Utrecht, EAERE 2024 conference, Leuven, EEA 2024 conference, Rotterdam, SURED 2024 conference, Ascona, T2M 2024 conference, Amsterdam, DGF 2025 conference, Hagen, as well as a workshop on macroeconomic models of climate change at the University of Freiburg for very helpful comments and suggestions. All remaining errors are our own.

1. Introduction

A cornerstone of climate policy is the social cost of carbon (SCC), defined as the expected present discounted value of all current and future damages from emitting one ton of carbon today. Rennert et al. (2022) use improved probabilistic socioeconomic projections, climate models, damage functions, and discounting methods to consistently value risk, and obtain a preferred mean estimate of \$185/tCO_2 for the SCC based on a near-term risk-free discount rate of 2%/year. This is 3.6 times higher than the US government's current value of \$51/tCO_2.[1] Adding all the economic, climatic and damage uncertainties, such as climate-related disasters and climate tipping points,[2] thus substantially increases the SCC. We analyse the significance of these external effects in a calibrated model.

Taking account of the effects of recurrent climate disasters and climate tipping points on the optimal risk-adjusted SCC (e.g., Lemoine and Traeger, 2016b, Cai and Lontzek, 2019, Hambel et al., 2021a) requires solving Hamilton–Jacobi–Bellman equations, which are notoriously difficult to solve, especially if they involve many state variables. Monte-Carlo methods for obtaining the optimal SCC are cheaper but give misleading results (Jensen and Traeger, 2014). To properly allow for skewed distributions of shocks with gradual arrival of impacts to the climate system and damages and of temperature-dependent disasters and irreversible climate tipping points is still mostly uncharted territory. Analytical expressions for the optimal SCC can yield qualitative insights and understanding that complement those from numerical optimisation. This is not a trivial undertaking, since the SCC must take account of a wide range of uncertainties regarding the evolution of the economy, temperature, and global warming damages.

Our rule pinpoints the different drivers of the optimal SCC: risk aversion, intertemporal substitution, time preference, the damage ratio, the expected arrival times of climate disasters and climate tipping, the expected losses after a climate disaster or climate tipping point, and aggregate economic activity. We can thus precisely pinpoint why some authors get different estimates. Integrated assessment studies make very different assumptions and yield, not surprisingly, very different estimates of the optimal SCC. Although much of the debate has centred on the choice of the utility discount rate (or pure rate of time preference), differences persist in assumptions about the economic growth rate, its distribution, and about the stochastic properties of the climate system and of global warming damages. The consequences of these assumptions remain relatively unexplored. It is not always clear where these differences come from.

To shed light on these issues, we derive an intuitive rule for the SCC that highlights the drivers of the SCC under various types of uncertainty. This rule means that the computational task of solving a complex stochastic dynamic programming problem numerically is avoided. Further, such a rule makes it easy to communicate with policymakers

[1] The estimate of \$185/tCO_2 incorporates updated scientific understanding throughout all components of the SCC in the open-source Greenhouse Gas Impact Value Estimator (GIVE) model, and responds to the near-term recommendations by the National Academies of Sciences, Engineering, and Medicine.

[2] Examples of climate tipping points are disintegration and melting of the Greenland and West Antarctic ice sheets, the breakdown of the Atlantic meridional overturning circulation, and the melting of the permafrost.

how preferences, attitudes to risk, and the various types of uncertainty affect the SCC. The rule shows how the SCC is affected by the adverse impact of global warming on aggregate output, the risk of recurring climate-related disasters, and the risk of irreversible climate tipping points. We have three objectives.

First, we seek a tractable approximate expression for the optimal risk-adjusted SCC that internalises (1) the global warming externality resulting from the effect of global warming on total factor productivity, (2) the risk of recurring climate-related disasters, and (3) the risk of irreversible cascading climate tipping with long lags for the full impact of tipping to materialise, for a stochastic AK model of the economy and the climate. To solve the Hamilton–Jacobi–Bellman equations that are needed to calculate the optimal SCC, we use perturbation methods. van den Bremer and van der Ploeg (2021) have used these methods before to obtain a rule for the optimal SCC that only allows for externality (1), but not for externalities (2) and (3). Recurring climate disasters contribute 70% to the SCC of \$172/tCO_2 for a growth- and risk-adjusted discount rate of 2%/year, and the relative contribution of climate tipping points accounts for about 9% of this SCC.

Second, we compare the accuracy of the rule for the optimal SCC with the numerical optimum obtained by a finite-difference method under a wide range of circumstances. We show that the rule works well, thus eliminating the computational burden of finding optimal climate policy numerically and giving additional insights into the drivers of the SCC. The rule not only performs well when only internalising externality (1), but also when internalising externalities (2) and (3). We find that the relative contribution of recurrent disaster risks in the SCC is largely unaffected by the discount rate, while that of climate tipping (productivity damages) is higher (lower) for low discount rates. Our rule for the optimal SCC is more accurate if damages are a small fraction of GDP, the risk of climate-related disasters does not react too strongly to temperature, and the risk of climate tipping is small.

Third, we examine the robustness of our rule by testing its accuracy *outside* the model for which it has been derived; e.g., by allowing for a falling cost of fossil fuel and a two-sector model of economic growth. To ease comparison, we apply the same calibration strategy. The rule for the optimal SCC, even though designed for a simpler one-sector model with a constant cost of fossil fuel, remains surprisingly accurate, which demonstrates the high robustness of our rule. The rule also works well with an exponential disaster intensity, stochastic shocks to the climate system, and a more general climate tipping model. In all these cases, our rule does not exhibit one or more characteristics of the model under consideration and yet provides a robust approximation to the optimal SCC if we remain in the model class of endogenous growth models. However, our rule is less accurate when we apply it to an exogenous growth model with sluggish recovery of the capital stock.

To make headway, we first modify the DSGE model of global warming and the economy of van den Bremer and van der Ploeg (2021) by replacing the model of carbon stock and temperature dynamics by a model in which temperature rises linearly in cumulative emissions. This temperature model captures the results from complex climate models well (Allen et al., 2009, Matthews et al., 2009, Dietz and Venmans, 2019), is used in policy analysis by the Intergovernmental Panel on Climate Change (IPCC), and avoids the problem of excessive inertia in the temperature response that well-known integrated assessment models of climate change and the economy suffer from (Dietz et al., 2021b).

We then extend our earlier approach to macroeconomic uncertainty by including risks of rare macroeconomic disasters (Barro, 2006, 2009, Barro and Jin, 2011) as well as normally distributed shocks to economic growth. Together with Epstein-Zin preferences, this helps to better match the observed risk-free rate and equity risk premium.[3] We allow global warming to negatively impact total factor productivity (Barrage and Nordhaus, 2024) but also to increase the risks of recurring climate-related disasters and irreversible climate tipping points. The latter allows for irreversible shifts to higher transient climate responses to cumulative emissions at an unknown future date.

Gourio (2012) models disaster risk as an adverse productivity shock or a "depreciation shock" to the capital stock, where these shocks can be either permanent and/or transitory, and the sizes and their arrival rates can be stochastic. The high-impact, low-probability nature of rare disasters poses challenges for numerical and perturbation methods solutions (Fernández-Villaverde and Levintal, 2018). However, if disasters destroy the growth rates of capital and productivity so that the same proportion is destroyed and the time variation of the effect of the disaster is the same, Gourio (2012) shows that the solution is more tractable as the disaster event is no longer a state variable (for disasters with time-varying impact). Only the disaster probability must be retained, and the solution can be made stationary using one common (non-stationary) growth rate.

Our model differs from Gourio (2012) in several ways. Our disasters are modelled as compound Poisson processes, so that disasters occur randomly according to a Poisson process, and the size of each jump is also a random variable. Unlike Gourio (2012), who models the arrival rate of disasters as an AR(1) process, we take this rate to be independent of previous disasters. Further, the size of our disasters shocks is distributed according to a (non-time-varying) power distribution, and our disasters are purely transitory (that is, fully localised in time), whereas Gourio (2012) employ a combination of normally distributed shocks during "disaster times", each of which converges to a long-run value over time. Gourio (2012) is thus able to model the term structure in the risk-premium and the transient response to disasters. Our risk premium is constant over time and does not respond to the occurrence of a disaster. Instead, our risk premium depends on temperature and thus on time. However, in assuming a production function of the AK-type, the stochastic properties of output and capital variables are the same, and thus we invoke Gourio's "trick". All our variables have the same growth rate, which does not vary through the transient response to disasters as in Gourio (2012) but instead through its dependence on time-varying climate variables (temperature).

[3] Disaster risk models offer tractable and parsimonious explanations to several asset pricing puzzles in equity and bond markets (Gabaix, 2012, Tsai and Wachter, 2015). This model class explains several stylised facts on equity and bond premia with moderate degrees of relative risk aversion of 3 to 6. Moreover, recent empirical evidence shows that disaster risk predicts bond excess returns both in- and out-of-sample (Su et al., 2022). Other popular models with long-run risk require additional state variables and much higher values of risk aversion that can easily exceed 10 (e.g., Bansal and Yaron, 2004) or state-dependent risk-aversion with much higher average values (Rudenbusch and Swanson, 2012).

Our rule for the optimal SCC in the absence of climate tipping risk is given in Result 1. It internalises the adverse effect of global warming on total factor productivity and on the expected loss of climate-related disasters. These terms and thus the optimal SCC are proportional to the transient climate response to cumulative emissions and to aggregate economic activity, increases in the damage coefficient for output damages and the risk-adjusted loss of a recurring climate disaster, and is inversely proportional to the risk- and growth-adjusted discount rate. The optimal SCC with risk of climate tipping is given in Result 2 and has an additional repricing term to take account of the probability that at some uncertain future time the transient climate response to cumulative emissions jumps up and a further term to internalise the adverse effect of global warming on the risk of climate tipping itself.

Our analysis builds on simple rules for the optimal SCC from *deterministic* growth models of climate and the economy. For example, Nordhaus (1991) derives an *approximate* rule for the optimal SCC under certainty, which is proportional to aggregate economic activity. Golosov et al. (2014) obtain a similar rule and give conditions under which the rule yields the *exact* welfare-maximising outcome in a DGSE framework.[4] Barrage (2014), van den Bijgaart et al. (2016), Rezai and van der Ploeg (2016), Hambel et al. (2021b) and Traeger (2023) perform a detailed numerical analysis of the performance of such approximate rules for the SCC under certainty and show that these are generally good approximations. Withagen (2022) discusses these rules and the insights they provide.

We follow Lemoine (2021), van den Bremer and van der Ploeg (2021), and Traeger (2025) and derive approximate, intuitive rules for the optimal SCC *under uncertainty* using *stochastic* integrated assessment, general equilibrium models of the economy and the climate. Our main innovation is that we have recurring temperature-dependent risks of recurring disasters and risks of irreversible climate tipping points. We also have standard forms of macroeconomic uncertainty (exogenous risk of rare macroeconomic disasters as well as Brownian shocks), while the recent papers of Traeger (2023, 2025) abstract from economic shocks and do not relate their model to financial markets.[5] Our rule for the SCC thus internalises the three externalities resulting from emissions curbing economic production, increasing the frequency of climate-related disasters, and bringing forward the expected date of a climate tipping point. Our quantitative results indicate that recurring climate disasters contribute at least 70% to the SCC, so ignoring this component leads to seriously misleading results.

Lemoine and Traeger (2014) put forward a climate tipping model that allows for learning about a threshold's location by observing the system's response in each period.

[4]These are logarithmic utility, Cobb–Douglas production, 100% depreciation of capital each period, a linear two-box model for the dynamics of atmospheric carbon, and damages to the logarithm of total factor productivity rising linearly in atmospheric carbon. This *exact* expression for the deterministic rule is extended to more general settings with a negative linear effect of atmospheric carbon on utility, mean reversion in the effects of damages on total factor productivity, less than 100% logarithmic depreciation, and policy makers who are more patient than private agents by van der Ploeg and Rezai (2022).

[5]Notably Traeger (2025) extends the deterministic model developed by Traeger (2023) and studies a model with various persistent shocks to the carbon cycle and the climate system. Traeger (2025) shows that those persistent climate shocks boost the optimal SCC.

We do not have learning, but deal with the optimal policy response to the possibility of *gradual* rather than *abrupt* irreversible shifts in system dynamics. Barnett et al. (2020, 2021) allow for risk from random shocks to the economy or the climate, but also for ambiguity resulting from multiple models with weights attached to each model updated in a Baysesian manner and for potential misspecification arising from the complexity of the economy and the climate to be understood. These latter two features are the cornerstones of robust control based on Hansen and Miao (2018) (the continuous-time equivalent of Hansen and Sargent (2007)). Our results do not allow for ambiguity or model misspecification, which we leave for further research.

Section 2 presents our stochastic integrated assessment model. Section 3 derives solutions to the model (in terms of the value function) using perturbation methods. These solutions are used in Section 4 to derive approximate rules for the optimal SCC that take account of the three global warming externalities, considering the scenarios without (Section 4.1) and with gradual climate tipping (Section 4.2) in turn. Section 5 discusses our calibration. Section 6 evaluates the numerical accuracy of our rules for the SCC by comparing them to the SCC obtained from full numerical optimisation. Section 7 road-tests the numerical accuracy of our rules for the optimal risk-adjusted SCC in more general models than have been used to derive the rule. Section 8 concludes.

2. Stochastic Integrated Assessment Model

We specify a macroeconomic DSGE model with endogenous growth and add fossil fuel as a production factor whose combustion gives rise to global warming.

Recursive Preferences The pure rate of time preference (or utility discount rate) is denoted by $\rho \geq 0$. The coefficient of relative risk aversion is denoted by $\gamma \geq 0$, the coefficient of intergenerational inequality aversion by $\eta \geq 0$, and the elasticity of intertemporal substitution by $1/\eta$. We use Epstein–Zin preferences to distinguish relative risk aversion, γ, from the inverse of the elasticity of intertemporal substitution, $1/\eta$ (Epstein and Zin, 1989).[6] We use continuous-time recursive preferences (Duffie and Epstein, 1992):

$$J_t = \mathbb{E}_t \left[\int_t^\infty f(C_s, J_s) \mathrm{d}s \right] \quad \text{with} \quad f(C_t, J_t) = \frac{1}{1-\eta} \frac{C_t^{1-\eta} - \rho[(1-\gamma)J_t]^{\frac{1-\eta}{1-\gamma}}}{[(1-\gamma)J_t]^{\frac{1-\eta}{1-\gamma}-1}}, \tag{1}$$

where the recursive aggregator $f(C_t, J_t)$ depends on aggregate consumption C_t and the value function J_t. If aversion to risk is the same as that to intertemporal fluctuations, $\gamma = \eta$, the aggregator function becomes $f(C_t, J_t) = \frac{C_t^{1-\gamma}}{1-\gamma} - \rho J_t$, and gives CRRA utility.

[6]Empirical evidence suggests $\gamma > \eta$, which reflects a preference for early resolution of uncertainty (Vissing-Jørgensen and Attanasio, 2003). Much of the macro-finance literature sets $1/\eta > 1$, so that macroeconomic volatility depresses share prices (Bansal and Yaron, 2004, Barro, 2009). Other empirical evidence suggests $1/\eta < 1$ (Hall, 1988, Campbell, 1999, Vissing-Jørgensen, 2002), which is also common in climate economics (e.g., Nordhaus (2007), Gollier (2018)).

Capital Dynamics The dynamics of the aggregate capital stock, denoted by K_t, is

$$\mathrm{d}K_t = \Big[I_t - \delta K_t - \frac{1}{2}\varphi\frac{I_t^2}{K_t}\Big]\mathrm{d}t + K_t\sigma \mathrm{d}W_{kt} - K_{t-}\ell_e \mathrm{d}N_{et} - K_{t-}\ell_c \mathrm{d}N_{ct}, \quad (2)$$

where I_t denotes aggregate investment, $\delta \geq 0$ the depreciation rate of capital, φ the parameter for investment adjustment costs, W_{kt} a Wiener process modelling economic shocks, $\sigma \geq 0$ the relative volatility of capital, and K_0 the initial capital stock. N_{et} is a Poisson point process capturing the risk of macroeconomic disasters that are independent of climate change. N_{ct} is another Poisson point process that models climate-related disaster shocks. The parameters $\ell_e \geq 0$ and $\ell_c \geq 0$ indicate the relative sizes of the jumps, which are stochastic but independent of N_{et}, N_{ct}, and W_{kt}. The recovery rate $Z_i \equiv 1 - \ell_i$ follows a power distribution with parameter β_i, so its probability density function is $f_i(Z_i) = \beta_i Z_i^{\beta_i - 1}$ with $Z_i \in (0, 1)$, where $\mathbb{E}[Z_i] = \frac{\beta_i}{\beta_i+1}$ for i is e or c. The jump intensity of N_{et} is constant and denoted by λ_e. The expected time until the next disaster is $1/\lambda_e$. The jump-intensity of N_{ct} depends on global warming and is denoted by $\lambda_c(T)$.[7]

Production The final goods production function is $Y_t = AK_t^{\alpha}F_t^{1-\alpha}$, where $0 < \alpha < 1$ and total factor productivity A is assumed to depend on global warming.[8] [9] Aggregate investment is $I_t = Y_t - C_t - bF_t$, where Y_t is aggregate production, F_t fossil-fuel use, and b the fixed production cost per unit of fossil fuel. In equilibrium, our model behaves like an AK model for endogenous growth (see Section 3), which does not allow for recovery after disasters. This is in line with empirical evidence that shows the absence of such recovery for macroeconomic disasters in general (Cerra and Saxena, 2008) and natural disasters in particular (Hsiang and Jina, 2014). The AK-model is thus used to model the effect of disasters on long-run growth (cf. Douenne, 2020). The aggregate consumption stream generated by AK models and the consumption streams that are typically used in the consumption-based asset pricing literature have similar characteristics. In particular, our AK model generates a consumption stream similar to that of Wachter (2013), see also Pindyck and Wang (2013) for an example without state variables.

[7]Using a suitably defined limit, it can be shown that climate disasters behave as if there is a permanent negative effect on capital growth when they are of high marginal jump-intensity and small jump size. Since output is proportional to capital in our model, climate disasters would appear as a growth rate impact, as was first empirically established by Dell et al. (2009, 2012) and in theoretical studies by Pindyck (2012), Moore and Diaz (2015), Hambel et al. (2021a), among others. The proof is available upon request.

[8]This production function stems from $Y = AK^{\beta}F^{1-\alpha}(K_aL)^{\alpha-\beta}$, where L denotes labour employed (without loss of generality set to 1), K_a denotes the economy-wide capital stock, and $0 < \beta < 1$. The economy-wide capital stock thus boosts the efficiency of labour, leading to a growth externality. In equilibrium, all firms are the same, so that the individual capital stock equals the economy-wide capital stock, $K = K_a$, and we have $Y = AK^{\alpha}F^{1-\alpha}$. The exponents of K and F add up to one, so there is endogenous growth. A production subsidy internalises the growth externality. We allow for technical progress in Section 7. We also abstract from labour-augmenting technical progress and population growth. Neither extension affects the derivation of our estimate of the optimal SCC presented in Results 1 and 2.

[9] It is easy to have renewable energy as a factor input. We assume that this is already optimised out and captured in A. An alternative is to let energy be a CES aggregate of renewable energy and fossil fuels (Golosov et al., 2014, Hambel and van der Ploeg, 2025). This has no direct influence on our simple rules.

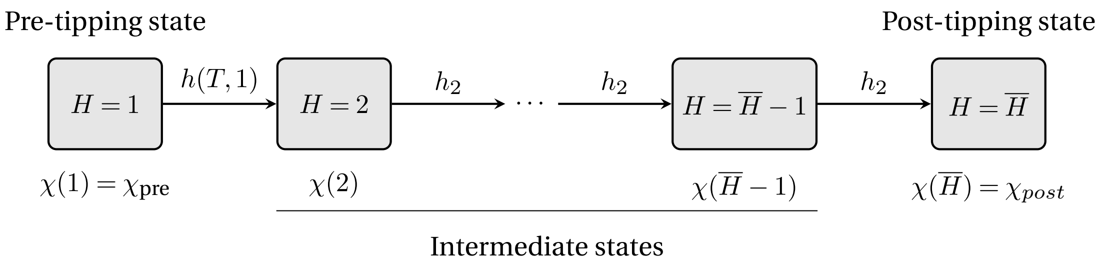

FIGURE 1. Structure of the Gradual Climate Tipping Process. *Note*: The figure illustrates how climate tipping propagates from a pre-tipping state $H = 1$ through several intermediate states to a post-tipping state $H = \overline{H}$ with $\chi_{\text{post}} > \chi_{\text{pre}}$ and how this gradually increases the TCRE.

Cumulative Emissions The emissions rate is $\varpi_t F_t$, where the emissions intensity, ϖ_t, falls due to technical progress at the rate of economic growth: $\varpi_t = \exp(-\int_0^t g_s \mathrm{d}s)$. Cumulative emissions denoted by E_t follow from

$$\mathrm{d}E_t = \varpi_t F_t \mathrm{d}t, \tag{3}$$

where E_t is measured from the start of the industrial era.

Global Warming and Climate Tipping Risk The temperature anomaly is the difference in temperature since pre-industrial times and is referred to as temperature T_t. It is driven by cumulative emissions since time zero, denoted by E_t, so that

$$T_t = \chi(H_t) E_t \tag{4}$$

with $\chi > 0$ the transient climate response to cumulative emissions (TCRE). Since temperature responds immediately to cumulative emissions, we do not have excessive inertia in the temperature response to marginal emissions, for which the main integrated assessment models used by economists have been criticised (Dietz et al., 2021b).[10]

To take account of irreversible climate tipping points and feedback loops in the climate system, we model a directed Markov chain H_t that takes values in a finite set $\{1, \ldots, \overline{H}\}$ of climate states (e.g., Cai et al., 2016, Cai and Lontzek, 2019). The climate system starts at $t = 0$ in the pre-tipping state $H_0 = 1$ with $\chi(1) = \chi_{\text{pre}}$ and eventually transitions to a post-tipping state $\overline{H}$ with $\chi(\overline{H}) = \chi_{\text{post}} > \chi_{\text{pre}}$.[11] Crossing such a tipping point induces further warming that takes time to manifest. This lag is modelled by the intermediate states $2, \ldots, \overline{H} - 1$. Once tipping has begun, the intermediate states are passed through one after the other until the post-tipping state of the climate system is reached.

[10] Building on Nordhaus (1992), other papers such as van den Bremer and van der Ploeg (2021) and Hambel et al. (2021a) use a more sluggish climate system that is exposed to stochastic shocks to the equilibrium climate sensitivity.

[11] While Cai and Lontzek (2019) assume that climate tipping affects the damage parameter of the model, we assume that climate tipping has a positive effect on the TCRE and thus on global average temperature.

In line with Cai and Lontzek (2019), we assume that tipping is only possible if temperature exceeds a certain safe threshold T^*. The hazard rate (or transition intensity) of a transition from the pre-tipping state 1 to the first intermediate state 2 is $h_t = h_{1T}\max(T_t - T^*, 0)$ with $h_{1T}, T^* \geq 0$. Using equation (4), the hazard rate for climate tipping becomes

$$h(E_t, 1) = h_{1T}\max(\chi_{\text{pre}}E_t - T^*, 0). \tag{5}$$

We follow Cai and Lontzek, 2019 and assume a constant transition intensity for all subsequent tipping states, i.e., $h(E_t, H_t) = h_{2T}$ is constant for $H_t = 2, \ldots, \overline{H}-1$. As the post-tipping state $\overline{H}$ is absorbing, we set $h(E_t, \overline{H}) = 0$.[12] Figure 1 visualises this Markov chain.

Climate Disasters and Damages Following Karydas and Xepapadeas (2022), the risk of climate-related disasters increases linearly in temperature, that is, $\lambda_{c,t} = \lambda^c_{0T} + \lambda^c_{1T}T_t$ with $\lambda^c_{1T} \geq 0$. Using equation (4), $\lambda^c_0 \equiv \lambda^c_{0T} + \lambda^c_{1T}T_0$ and $\lambda^c_1(H_t) \equiv \chi(H_t)\lambda^c_{1T}$, the jump intensity for the point process N_c becomes

$$\lambda_c(E_t, H_t) = \lambda^c_0 + \lambda^c_1(H_t)E_t, \tag{6}$$

where $\lambda_c \mathrm{d}t$ is the probability of a jump to occur in the infinitesimally small time interval $\mathrm{d}t$. Global warming affects the arrival rate of climate-related disasters but not the distribution of the size of these disasters. Global warming induces proportional losses in total factor productivity, $A_t \equiv A^*(1 - D_t)$, where the damage ratio, $D_t = D_0 + D_{1T}T_t$ with $D_{1T} \geq 0$, rises linearly in temperature. The marginal effect of temperature on the damage ratio is thus D_{1T}. With $D_1 \equiv \chi(H_t)D_{1T}$, being the marginal effect of carbon on the damage ratio, the reduced-from damage ratio and total factor productivity are

$$D(E_t, H_t) = D_0 + D_1(H_t)E_t, \qquad A(E_t, H_t) = A^*\big[1 - \big(D_0 + D_1(H_t)E_t\big)\big]. \tag{7}$$

The damage ratio rises while total factor productivity falls in cumulative emissions. Finally, the parameters in the equations for $\lambda_c(E_t, H_t)$, $D(E_t, H_t)$, and $h(E_t, H_t)$, including the pre- and post-tip values of the TCRE, are known and not stochastic.[13]

3. Value Function Solutions: Perturbation Methods

The optimal solution must satisfy the Hamilton-Jacobi-Bellman (HJB) equation,

$$0 = \max_{C,F}\Big[f\big(C, J\big) + J_K\Big[A(E,H)K^\alpha F^{1-\alpha} - C - bF - \delta K - \frac{1}{2}\varphi\frac{I^2}{K}\Big] + \frac{1}{2}J_{KK}K^2\sigma^2$$

[12] Some authors assume that the climate system is driven by normally distributed shocks (e.g., Hambel et al., 2021a, Barnett et al., 2021, Barnett, 2023). We abstract from this additional layer of complexity since it neither affects our analytical results nor does it have a significant influence on their numerical accuracy. It has, however, the advantage that it prevents the climate system from inevitably tipping once the threshold T^* has been crossed. Moreover, the Markov chain can also be generalised to a setting with multiple absorbing states. For instance, the introduction of a non-tipping state, i.e., a second absorbing state state can only be reached from the pre-tipping state, allows us to model the possibility that tipping never happens. Our results are robust with respect to these two extensions, see Section 7.

[13] Results with stochastic shocks to the damage ratio and the TCRE are available upon request. See van den Bremer and van der Ploeg (2021) for a discussion of the effects of such stochastic parameters.

$$+ J_E \varpi F + \lambda_c(E,H)\mathbb{E}\big[J\big((1-\ell_c)K,E,H\big) - J(K,E,H)\big] \tag{8}$$
$$+ \lambda_e \mathbb{E}\big[J\big((1-\ell_e)K,E,H\big) - J(K,E,H)\big] + h(E,H)\big[J(K,E,H+1) - J(K,E,H)\big]\Big],$$

where $J = J(K,E,H)$ denotes the value function. Optimality requires equalising the marginal values of consumption and investment,

$$f_C(C,J) = C^{-\eta}\big((1-\gamma)J\big)^{\frac{\eta-\gamma}{1-\gamma}} = J_K\Big(1 - \varphi\frac{I}{K}\Big), \tag{9}$$

and setting the marginal product of fossil fuel to its production cost, b, plus the SCC, i.e.,

$$(1-\alpha)\frac{Y}{F} = b + \varpi P, \tag{10}$$

where $P \equiv -J_E/f_C > 0$ denotes the optimal SCC. One way to implement the first-best outcome in a decentralised market economy is to set the carbon price to the SCC and rebate the revenue to the private sector as lump-sum payments. Since optimal use of fossil fuel is proportional to Y, we have, in equilibrium, an "AK" model of endogenous growth with the reduced-form aggregate production function,

$$Y = B(E,H,P)K, \tag{11}$$

where $B(E,H,P) \equiv \big[A(E,H)\big(\frac{1-\alpha}{b+\varpi P}\big)^{1-\alpha}\big]^{1/\alpha}$ and P depend on the states K, E, and H.

3.1 *Perturbation analysis*

To solve models with rare disasters with perturbation methods, one expands the model in a small parameter that corresponds to the volatility of the model, so that the zeroth-order solution corresponds to the deterministic model (Levintal, 2017, Fernández-Villaverde and Levintal, 2018). A perturbation up to and including third order in this small parameter can capture the effects of prudence and precautionary saving (Isoré and Szczerbowicz, 2017), but higher-order perturbations may be required if the disaster volatility has a term structure or large nonlinearities (Fernández-Villaverde and Levintal, 2018). The Taylor projection method proposed by Levintal (2018) and used in Fernández-Villaverde and Levintal (2018) uses a Taylor-series expansion to expand the policy functions as polynomial functions of the states around a certain point in state space, but still requires a numerical projection algorithm to solve these approximated policy functions (at considerably lower computational expense). It thus differs from a perturbation method. Isoré and Szczerbowicz (2017) employ the same "trick" as Gourio (2012) (see the introduction) in the context of a real business cycle model with rare disasters, and show that this limits the order of perturbation that is needed to capture the full non-linearities of the model to three. Fernández-Villaverde and Levintal (2018) do not employ this "trick" and thus require higher orders to be included in their perturbation analysis (beyond three).

Our zeroth-order solution (the solution we perturb around) is not a version of our model without volatility as in Levintal (2017) and Fernández-Villaverde and Levintal

(2018). Instead, our zeroth-order solution allows for normally distributed shocks and disaster risks, where both have constant (non-time-varying) effects on the growth rate, as the effects of future temperature increases are deemed to be negligible in the zeroth-order solution. In this sense, our zeroth-order solution can be thought of as a 'local' approximation of the value function in its climate-related states (but a 'global' unapproximated solution in the capital stock) that freezes the temperature evolution (and the marginal dependence of the value function on temperature) locally at its current value.

We outline the main steps and assumptions of our perturbation analysis here, but leave further details to Appendix A. After substitution of the optimality conditions (9) and (10), the HJB equation (8) can be written as

$$\mathcal{F}\left[J(\mathbf{x}),\mathbf{x}\right]=0, \tag{12}$$

where the 'operator' $\mathcal{F}$ is typically nonlinear, includes first- and second-order derivatives of the value function J with respect to the vector of states $\mathbf{x}$, which may include time, and is also a (nonlinear) function of $\mathbf{x}$ directly. We choose a (single) small parameter ϵ, defined so that we return to the simpler, exactly solvable problem (or the 'zeroth-order solution') in the limit as $\epsilon \to 0$.

To solve (12), we expand the operator $\mathcal{F}$ and the value function $J(\mathbf{x})$ as series in ϵ (cf. Van Dyke (1975), Kevorkian and Cole (1996), Bender and Orszag (1999), Nayfeh (2004)),

$$\mathcal{F}=\mathcal{F}^{(0)}+\epsilon\mathcal{F}^{(1)}+\mathcal{O}\left(\epsilon^2\right), \quad J(\mathbf{x})=J^{(0)}(\mathbf{x})+\epsilon J^{(1)}(\mathbf{x})+\mathcal{O}\left(\epsilon^2\right), \tag{13}$$

where $\mathcal{F}^{(0)}$ contains all operations that leave the order unchanged and $\epsilon\mathcal{F}^{(1)}$ contains all operations that increase the order by ϵ. For clarity, note that (13) is not a (multivariate) Taylor series expansion in the (vector of) state variables $\mathbf{x}$, which would require at least three orders of expansion to capture the effects of risk aversion and prudence and would rapidly become cumbersome. Instead, the individual terms in (13) retain a fully nonlinear (unapproximated) dependence on the state variables $\mathbf{x}$, whilst only approximately capturing the effects that depend on the small parameter ϵ. Substituting equation (13) into (12), expanding, and subsuming the term $\epsilon^2\mathcal{F}^{(1)}J^{(1)}$ in $\mathcal{O}(\epsilon^2)$ gives

$$\mathcal{F}^{(0)}\left[J^{(0)}(\mathbf{x}),\mathbf{x}\right]+\epsilon\left(\mathcal{F}^{(0)}\left[J^{(1)}(\mathbf{x}),\mathbf{x}\right]+\mathcal{F}^{(1)}\left[J^{(0)}(\mathbf{x}),\mathbf{x}\right]\right)+\mathcal{O}(\epsilon^2). \tag{14}$$

We thus solve the zeroth-order value function $J^{(0)}$ from $\mathcal{F}^{(0)}\left[J^{(0)}(\mathbf{x}),\mathbf{x}\right]=0$ at order $\mathcal{O}(1)$ (see Section 3.2), and then use this to solve for the first-order value function $J^{(1)}$ from $\mathcal{F}^{(0)}\left[J^{(1)}(\mathbf{x}),\mathbf{x}\right]+\mathcal{F}^{(1)}\left[J^{(0)}(\mathbf{x}),\mathbf{x}\right]=0$ at order $\mathcal{O}(\epsilon)$ (see Section 3.3). The first-order value function thus corrects the zeroth-order value function to allow for the effect of cumulative emissions on the economy with an error that is $\mathcal{O}(\epsilon^2)$. (This can be corrected by $\epsilon^2 J^{(2)}(\mathbf{x})$ (with an error that is $\mathcal{O}(\epsilon^3)$) and so forth.)

What is crucial is whether a single or multiple small parameters can be found for our model. Using a process known as non-dimensionalisation, which is standard in the physical sciences, we obtain several non-dimensional numbers (or parameters) that measure the importance of different effects in the model relative to each other (see Appendix A.1). Of these non-dimensional numbers, we set the majority to be $\mathcal{O}(1)$, so the effects they represent are included in the solution of the model without approximation (i.e., they are not small). For Result 1 to be valid, we require the non-dimensional numbers

$$\hat{D}_1 = \frac{D_{1T}\chi_{\text{pre}}F_0}{g_0(1-D_0)} = \mathcal{O}(\epsilon), \qquad \hat{\lambda}_1^c = \frac{\lambda_{1T}^c \chi_{\text{pre}} F_0 \mathbb{E}[\ell_c]}{g_0^2} = \mathcal{O}(\epsilon) \tag{15}$$

to be small (see Appendix A.1). The small parameter $\hat{D}_1$ measures climate damages relative to GDP for (new) cumulative emissions, which is typically small relative to other components of the model (cf. van den Bremer and van der Ploeg (2021)), and $\hat{\lambda}_1^c$ measures the dependence of the expected loss from recurring disasters due to new (cumulative) emissions relative to the economic growth rate. For Result 2 to be valid, we need $\hat{h} = h/g_0$ to be small. This requires three additional small parameters:

$$\hat{h}_{0,\text{pre}} = \frac{h_{1T}(T_0 - T^*)}{g_0} = \mathcal{O}(\epsilon), \quad \hat{h}_1 = \frac{h_{1T}\chi_{\text{pre}}F_0}{g_0^2} = \mathcal{O}(\epsilon), \quad \hat{h}_{0,\text{post}} = \frac{h_{2T}}{g_0} = \mathcal{O}(\epsilon). \tag{16}$$

Finally, we have set all five small parameters to be equally small, i.e., to be of the same order of magnitude in ϵ. Note that the small parameters are non-dimensional, i.e., they do not have units.[14] We return to whether the five small parameters are indeed quantitatively small for typical values used in our calibration in Section 5.4.

3.2 *Zeroth-order solution*

It can be shown that the zeroth-order solution takes the form (see Appendix A.3)

$$J^{(0)}(K,E,H) = \frac{1}{1-\gamma}K^{1-\gamma}\psi^{(0)}(E,H) \text{ with } \psi^{(0)}(E,H) = \frac{\left(r^\star(E,H)\right)^{\frac{-\eta(1-\gamma)}{1-\eta}}}{\left(1-\varphi i^{(0)}(E,H)\right)^{1-\gamma}}, \tag{17}$$

where the solution depends on the climate states E and H but the effect of their (future) variation has not been taken into account yet (this will be captured at the next order by $J^{(1)}(K,E,H)$). The climate variables E and H have thus been assumed constant to derive the zeroth-order solution. The (zeroth-order accurate) discount rate $r^\star$ is

$$r^\star(E,H) = \rho + (\eta-1)\Big[g^{(0)}(E,H) - \tfrac{1}{2}\gamma\sigma^2 - \frac{\lambda_e}{1-\gamma}\mathbb{E}\big[1-Z_e^{1-\gamma}\big] - \frac{\lambda_c(E,H)}{1-\gamma}\mathbb{E}\big[1-Z_c^{1-\gamma}\big]\Big], \tag{18}$$

[14]The first small parameter $\hat{D}_1$ combines D_{1T} (%/°C), χ_{pre} (°C/GtC), and F_0 (TtC/year) in the numerator with g_0 (%/year) and D_0 (already non-dimensional) in the denominator. The second small parameter $\hat{\lambda}_1^c$ combines λ_{1T}^c (%/°C), χ_{pre} (°C/GtC), F_0 (TtC/year), and $\mathbb{E}[\ell_c]$ (already non-dimensional) in the numerator with the square of g_0 (%/year) in the denominator. The third small parameter $\hat{h}_{0,\text{pre}}$ combines h_{1T} (%/°C), T_0 (°C), and T^* (°C) in the numerator with g_0 (%/year) in the denominator. The fourth small parameter $\hat{h}_1$ combines h_{1T} (%/°C), χ_{pre} (°C/GtC), and F_0 (TtC/year) in the numerator with the square of g_0 (%/year) in the denominator. The fifth small parameter $\hat{h}_{0,\text{post}}$ combines h_{2T} (%/year) in the numerator with g_0 (%/year) in the denominator.

and the investment rate $i^{(0)} = I_t^{(0)}/K_t$, which is needed to evaluate $g^{(0)} = i^{(0)} - \delta - \frac{1}{2}\varphi\left(i^{(0)}\right)^2$, follows from the (nonlinear) implicit equation

$$i^{(0)}(E,H) + \frac{r^\star(E,H)}{1-\varphi i^{(0)}(E,H)} = \alpha\left(\frac{b}{1-\alpha}\right)^{1-\frac{1}{\alpha}} A(E,H)^{1/\alpha}, \tag{19}$$

Together, equations (17)-(19) correspond to the solution of the model of Pindyck and Wang (2013) but with an additional dependence on the climate states E and H.

3.3 *First-order solution*

It can be shown that the first-order solution takes the form (see Appendix A.4)

$$J^{(1)}(K,E,H) = \frac{1}{1-\gamma}K^{1-\gamma}\psi^{(1)}(E,H), \tag{20}$$

$$\epsilon\psi^{(1)}(E,H) = h(E,H)\frac{\psi(E,H+1)-\psi^{(0)}(E,H)}{r^\star(E,H)}, \tag{21}$$

where $\psi^{(0)}(E,H)$ and $r^\star(E,H)$ are obtained from the zeroth-order solution in Section 3.2, and ψ is recursively defined by $\psi(E,H) = \psi^{(0)}(E,H) + \frac{h(E,H)}{r^\star}\left(\psi(E,H+1) - \psi^{(0)}(E,H)\right)$, $\psi(E,\overline{H}) = \psi^{(0)}(E,\overline{H})$. Note that $J^{(1)}(E,\overline{H}) = 0$, since the final tipping state is an absorbing state, and our model without tipping does not have a (non-zero) first-order solution. This follows from the linear dependence of damages and the hazard rate of disasters on cumulative emissions, but this can be generalised (see van den Bremer and van der Ploeg (2021), who do this for nonlinear damages but not for recurrent disasters or tipping).

4. The Optimal SCC

We now proceed by using the zeroth- and first-order value function solutions derived in Section 3 to obtain a leading-order estimate of the SCC.

4.1 *A rule for the optimal SCC without climate tipping*

Without climate tipping, a leading-order estimate of the optimal SCC can be obtained based on the zeroth-order solution alone, where the term 'leading order' refers to the lowest-order (and thus largest) term in the small parameter ϵ. For ease of notation, we drop the time subscripts t throughout this section. In this case, the Markov chain H is redundant, and the TCRE is just a constant $\chi = \chi_{pre}$.

Result 1. *Without risk of climate tipping, the leading-order approximation to the SCC is*

$$P_{\text{R1}} = \left[D_{1T} + \lambda_{1T}^c \frac{\mathbb{E}\left[1-Z_c^{1-\gamma}\right]}{1-\gamma}\frac{q^{(0)}}{B^{(0)}}\right]\frac{\chi Y^{(0)}}{r^\star}, \tag{22}$$

where the discount rate adjusted for risk and growth is given by

$$r^\star = \rho + (\eta - 1)\Big[g^{(0)} - \frac{1}{2}\gamma\sigma^2 - \frac{\lambda_e}{1-\gamma}\mathbb{E}\big[1 - Z_e^{1-\gamma}\big] - \frac{\lambda_c}{1-\gamma}\mathbb{E}\big[1 - Z_c^{1-\gamma}\big]\Big], \qquad (23)$$

$q^{(0)} = \frac{1}{1-\varphi i^{(0)}}$ *is Tobin's Q with* $i^{(0)}$ *the investment rate for the zeroth-order solution and* $g^{(0)}$ *expected growth not taking into account macroeconomic and climate-related disasters.*

Proof: Since reduced-form damages and the disaster hazard rate depend linearly on E, $J_E^{(1)} = 0$ holds and thus the estimate of the optimal SCC follows from $P_{\text{R1}} = (-J_E^{(0)}/J_K^{(0)})q^{(0)}$ and equations (17), (18), and (19) (see Appendix A.3). □

Only leading-order terms are retained for consistency. If the disaster sizes follow power distributions with parameters β_e and β_c (with $\beta_e, \beta_c > \gamma - 1$), the optimal SCC (22) becomes $P_{\text{R1}} = \big[D_{1T} + \frac{\lambda_{1T}^c}{\beta_c + 1 - \gamma}\frac{q^{(0)}}{B^{(0)}}\big]\frac{\chi Y^{(0)}}{r^\star}$, and (23) $r^\star = \rho + (\eta - 1)\big(g^{(0)} - \frac{1}{2}\gamma\sigma^2 - \frac{\lambda_c}{1+\beta_c-\gamma} - \frac{\lambda_e}{1+\beta_e-\gamma}\big)$.

To interpret Result 1, note that the two terms in the square brackets in (22) correspond to the expected marginal damage per unit of aggregate output from having one degree higher temperature. The term D_{1T} is the (expected) marginal effect of one degree higher temperature on the damage ratio D. The other term in the square brackets in (22) is the expected marginal loss of one degree higher temperature due to a higher risk of a rare recurring climate-related disaster. It is proportional to the marginal increase in disaster risk due to a higher temperature λ_{1T}^c, the TCRE χ, and the risk-adjusted expected disaster loss (as share of the capital stock) $\mathbb{E}[1 - Z_c^{1-\gamma}]/(1-\gamma)$. This risk-adjusted expected loss increases in relative risk aversion γ. To get the expected loss in units of lost output of final goods, it must be multiplied by $q^{(0)}/B^{(0)} = q^{(0)}K/Y^{(0)}$, where $q^{(0)}K$ represents the replacement costs to rebuild the capital stock.

We also observe from (22) that our estimate of the optimal SCC is proportional to the transient climate response to cumulative emissions χ, and to aggregate output of final goods $Y_t^{(0)}$.[15] Further, our estimate of the SCC is inversely proportional to the risk- and growth-adjusted discount rate $r^\star$ given in (23). This rate is used to discount all future marginal damages of emitting one ton of carbon today, taking account of normal macroeconomic uncertainties and the risk of recurring climate-related disasters and of marginal damages and losses due to climate disasters that grow in line with the economy.

Result 1 generalises van den Bremer and van der Ploeg (2021), which ignore temperature-related disaster risks in which case the result boils down to $P_{\text{R1}} = \frac{D_{1T}\chi Y^{(0)}}{r^\star}$. Result 1 contains an extra term to correct for the adverse effects of global warming on disaster risks. The optimal SCC is proportional to the aggregate capital stock or (due to the "AK" feature of our macroeconomic model) proportional to GDP.

[15]In fact, the optimal SCC is proportional to aggregate output that prevails in the absence of carbon pricing. This follows directly from our perturbation approximations.

Both components of the SCC in (22) decrease in the discount rate (23). Hence, for a constant growth rate $g^{(0)}$, a lower pure rate of time preference ρ implies a lower discount rate and a higher SCC.[16] If the coefficient of intergenerational inequality aversion η exceeds one, (22) and (23) indicate that lower economic growth and higher macroeconomic uncertainty, whether stemming from geometric Brownian motion or from negative climate-related disaster shocks, lower the discount rate and increase the SCC.

We can decompose the discount rate (23) if disasters follow a power distribution as

$$r^\star = \underbrace{\rho}_{\substack{\text{pure time}\\ \text{preference}}} \underbrace{+\eta g^{(0)}_{\text{total}}}_{\substack{\text{affluence}\\ \text{effect}}} \underbrace{-g^{(0)}_{\text{total}}}_{\substack{\text{growing}\\ \text{damages}}} \underbrace{-\frac{1}{2}(1+\eta)\gamma\sigma^2_{\text{total}}}_{\substack{\text{prudence}\\ \text{effect}}} \underbrace{+\gamma\sigma^2_{\text{total}}}_{\substack{\text{insurance}\\ \text{effect}}}, \tag{24}$$

where $g^{(0)}_{\text{total}} \equiv g^{(0)} - \lambda_e/(1+\beta_e) - \lambda_c/(1+\beta_c)$ is total expected growth, corrected for the expected negative effect of disasters, and

$$\sigma^2_{\text{total}} \equiv \sigma^2 + \frac{2\lambda_e}{(1+\beta_e)(1+\beta_e-\gamma)} + \frac{2\lambda_c}{(1+\beta_c)(1+\beta_c-\gamma)}$$

is a normal-equivalent measure of total uncertainty, combining normally distributed shocks with the effects of macroeconomic and climate-related disasters.[17]

The first two terms in (24) correspond to the deterministic Keynes–Ramsey rule: the rate of pure time preference ρ plus the affluence effect $\eta g^{(0)}_{\text{total}}$. The affluence effect captures that, if growth and aversion to intergenerational inequality aversion are high, policymakers postpone climate action when people are richer.[18] The third term $-g^{(0)}_{\text{total}}$ corrects the discount rate for growing output and damages, so that a higher growth rate increases the SCC. Together, the second and the third terms act to increase the discount rate and reduce the SCC if intergenerational inequality is high enough ($\eta > 1$).

The fourth term $-\frac{1}{2}(1+\eta)\gamma\sigma^2_{\text{total}}$ is the prudence term, which indicates that normally distributed and disaster risks necessitate precautionary saving. This depresses the interest rate and increases the SCC in equilibrium, especially for large degrees of relative risk aversion γ, relative prudence $1+\eta$, and macroeconomic volatility, $\sigma > 0$, $\lambda_c > 0$ and $\lambda_e > 0$. The fifth term $\gamma\sigma^2_{\text{total}}$ is the insurance effect. It stems from the perfect correlation between damages from macroeconomic and climate-related disasters on the one hand and output on the other hand: in future states of nature, damages are high if output and consumption are high and the marginal utility of consumption is low. Policymakers

[16]In contrast to exogenous Ramsey growth models such as Golosov et al. (2014) and Nordhaus (2017), our rate of economic growth $g^{(0)}$ is endogenous. Hence, there are indirect effects on the optimal SCC via the growth rate $g^{(0)}$. For example, the direct effect of a higher rate of pure time preference ρ is to lower the SCC and the indirect effect is to raise the SCC as economic growth is lowered (for $\eta > 1$). Together, we find that the effect of a higher rate ρ on $r^\star$ is always positive and on the SCC always negative.

[17]The coefficient of relative risk aversion γ appears in this measure of total uncertainty because of the non-normal nature of these shocks. As β_e and β_c are generally much larger than γ (see Section 5), the quantitative effect of γ on the SCC is relatively small.

[18]The increased desire to consume and save less requires a higher interest rate for household-investors to willingly hold the safe asset, which is in fixed supply.

thus employ a higher discount rate and undertake less climate action. This effect is large if relative risk aversion (γ) and macroeconomic volatility ($\sigma > 0$, $\lambda_c > 0$ and $\lambda_e > 0$) are large.

The equity premium and the risk-free rate We can use our model to price risk-free bonds and the claim to aggregate dividends along the lines of Pindyck and Wang (2013).[19] Without risk of climate tipping, the leading-order estimate of the equity premium and the risk-free rate are, respectively,

$$r_p = \gamma\sigma^2 + \sum_{i=e,c} \lambda_i \mathbb{E}\big[(1-Z_i)(Z_i^{-\gamma}-1)\big] \tag{25}$$

and

$$r_f = \rho + \eta g^{(0)} - \frac{1}{2}\gamma(1+\eta)\sigma^2 - \sum_{i=e,c} \lambda_i \mathbb{E}\Big[(Z_i^{-\gamma}-1) + \frac{\eta-\gamma}{1-\gamma}(1-Z_i^{1-\gamma})\Big]. \tag{26}$$

This result extends well-known expressions in the macro-finance literature to allow for temperature-dependent risk of climate-related disasters. Equation (23) can be written as

$$r^\star = r_f + r_p - g^{(0)}_{\text{total}}, \quad \text{where} \quad g^{(0)}_{\text{total}} \equiv g^{(0)} - \sum_{i=e,c} \lambda_i \mathbb{E}[1-Z_i]. \tag{27}$$

The discount rate $r^\star$ is the return on risky assets $r_f + r_p$ minus the growth rate that takes account of expected damages from disasters, $g^{(0)}_{\text{total}}$. Since the risk-free interest rate, the risky rate, and economic growth are observable, we can back out γ and η for a given ρ by matching asset-pricing moments. In Figure E.5 in Appendix E, we compare our leading-order estimate of $r^\star$ with its counterpart obtained from numerical simulations.

4.2 *A rule for the optimal SCC with gradual climate tipping*

RESULT 2. *With temperature-dependent risks of recurring climate-related disasters and irreversible gradual climate tipping, the optimal SCC in state $H = 1, \ldots, \overline{H}-1$ can be estimated recursively by*

$$\begin{aligned} P_{\text{R2}}(E,H) = {} & P_{\text{R1}}(E,H) + h_E(E,H)\frac{1}{r^\star}\frac{Kq^{(0)}}{\gamma-1}\Big(\frac{\psi(E,H+1)}{\psi^{(0)}(E,H)}-1\Big) \\ & + h(E,H)\frac{1}{r^\star}\Big(P_{\text{R2}}(E,H+1)\frac{\psi(E,H+1)}{\psi^{(0)}(E,H)} - P_{\text{R1}}(E,H)\Big), \end{aligned} \tag{28}$$

[19] The aggregate stock market is defined as the claim to aggregate dividends. The price of the dividend claim is thus $S_t = \mathbb{E}_t\big[\int_t^\infty \frac{H_s}{H_t} C_s \mathrm{d}s\big]$, where H_t denotes the stochastic discount factor or pricing kernel (e.g., Duffie and Epstein, 1992) and aggregate dividends equal aggregate consumption in equilibrium (e.g., Barro, 2009). The expected rate of return on the dividend claim is then $r_p + r_f$, where r_p is the equity premium and r_f is the risk-free interest rate. The calculations leading to equations (25) and (26) follow along the lines of Pindyck and Wang (2013).

where $P_{\mathrm{R1}}(E,H)$ is the leading order-approximation to the SCC in tipping state H according to (22), $q^{(0)}=q^{(0)}(E,H)$ denotes Tobin's Q, and $r^{\star}=r^{\star}(E,H)$ the growth-adjusted discount rate in tipping state H, all obtained from for the zeroth-order solution, and

$$\psi(E,H)=\psi^{(0)}(E,H)+\frac{h(E,H)}{r^{\star}}\big(\psi(E,H+1)-\psi^{(0)}(E,H)\big),\qquad \psi(E,\overline{H})=\psi^{(0)}(E,\overline{H}).$$

Proof: This result follows from $P_{\mathrm{R2}}=-\big(\frac{J_E^{(0)}+\epsilon J_E^{(1)}}{J_K^{(0)}}\big)q^{(0)}$ with the derivatives of the value function with respect to E now obtained from both the zeroth- and first-order solution (see Appendix A.4). □

If there is a risk of climate tipping in the pre-tipping state ($h(E,1)>0$), the anticipated future damages caused by a future upward jump in the transient climate response (TCRE) and the resulting higher temperatures need to be internalised.[20] Hence, the carbon price needs to be adjusted to mitigate the risk of a climate tipping point (second term in (28)), and carbon needs to be repriced to allow for the anticipated effect that the TCRE jumps up in the future (third term in (28)).[21] This calculation must be performed recursively starting from the post-tipping $\overline{H}$, since the markup terms in each state H depend on the carbon price in its successor state $H+1$. This recursion reflects the cascading behaviour of the climate system that starts once the tipping point has been crossed.

The second term in (28) only arises if the hazard rate of tipping is endogenous and is positive if the hazard rate of tipping increases with temperature. This is only the case in the pre-tipping state, where the hazard rate of tipping is given by (5), but not in the intermediate states. Since the economy is worse off after the irreversible climate tipping point, we have $\psi(E,2)>\psi^{(0)}(E,1)$.[22] The term captures the expected marginal loss from having one degree higher temperature. It implies that a larger dependence of the risk of irreversible climate tipping on temperature h_{1T} and a higher pre-tip TCRE χ, combining as $h_E(E,H)=\chi h_{1T}$ if $T>T^{*}$, and a larger risk-adjusted loss to welfare $\frac{1}{\gamma-1}\big(\frac{\psi(E,H+1)}{\psi^{(0)}(E,H)}-1\big)>0$ resulting from the tip increase the optimal SCC. Just as for the risk of recurring climate-related disaster risks, this effect is more pronounced if risk aversion is high (as captured by the risk-adjusted loss term).

The third term in (28) allows for the risk of climate tipping itself. It equals the tip arrival rate multiplied by the gap between the post-tip and the pre-tip SCC weighted by pre- and post-tip welfare, respectively, discounted at the pre-tip risk-adjusted discount

[20] If the arrival rate of tipping in the pre-tipping state is zero, $h(E,1)=0$, (28) reduces to Result 1.

[21] These adjustments correspond to two well-known effects that were first identified by Lemoine and Traeger (2014) and further investigated by Lemoine and Traeger (2016a). The second term corresponds to the *marginal hazard effect* (MHE) on welfare and the third term to the *differential welfare impact* (DWI). Result 2 discusses the influence of these effects on the SCC rather than on welfare and thus allows for an interpretation of these effects in monetary units.

[22] This follows from $\psi(E,H)=\psi^{(0)}(E,H)+\frac{h(E,H)}{r^{\star}}\big(\psi(E,H+1)-\psi^{(0)}(E,H)\big)$ as $\psi^{(0)}(E,H+1)>\psi^{(0)}(E,H)$.

rate. This term prices in that at some uncertain date in the future, the TCRE (χ) and thus damages jump up. This pushes up the optimal SCC (independent of whether the hazard rate of the climate tipping point is dependent on temperature and thus endogenous or not).

4.3 *Discussion of the perturbation analysis for Results 1 and 2*

The assumptions we make have consequences for the effects we include, exclude, or approximate. These assumptions fall into two categories: those that underlie the form of model we have chosen, which are tested in Section 7, and those that pertain to the solution method (perturbation methods), which we discuss here. Result 1, which can be derived from the zeroth-order solution for the value function, effectively relies on the assumptions that damages will remain a fraction of GDP and that the increase in impact of recurring climate disasters due to climate change will be small compared to the growth rate of the economy (cf. (15)). These assumptions have two consequences.

First, the flow of future marginal GDP and disaster damages from emitting one additional ton of CO_2 today (the numerator in Result 1) can be estimated from marginal GDP and disaster damages at today's temperature. Here, we also rely on the assumption that the damage ratio and the hazard rate of climate disasters are linear function of cumulative emissions (see also the special case of $\theta_{ET} = 0$ in van den Bremer and van der Ploeg (2021)). If damages and the hazard rate of recurring disasters are not proportional to the stock of cumulative emissions, emissions today would also affect future marginal GDP and disaster damages, which would need to be captured by additional first-order terms in the value function (see the first-order solutions underlying Result 2 in van den Bremer and van der Ploeg (2021)).

Second, the flow of future marginal (GDP and disaster) damages from emitting one additional ton of CO_2 today can be discounted using a discount rate (the denominator in Result 1) that includes a climate risk premium ('insurance effect') and a climate precaution premium ('prudence effect') estimated at today's temperature. The climate risk premium and the climate precaution premium associated with future increases in recurring disasters are thus assumed to be negligibly small. In line with this, Jensen and Traeger (2021) also find that their 'climate risk premium' is not primarily caused by the correlation between marginal damages and marginal utility.

Result 2, which can be derived from the combination of the zeroth and first-order solutions for the value function, additionally relies on the assumptions that the arrival rate of tipping is small relative to the growth rate of the economy and its marginal dependence on future temperature increases is small (and constant) (cf. (16)). As a consequence, the different contributions to Result 2 can simply be summed, and the discount rate can be approximated as being unaffected by tipping.

5. Market-Based Calibration

Our calibration strategy builds on Pindyck and Wang (2013), van den Bremer and van der Ploeg (2021), Karydas and Xepapadeas (2022), and Hambel et al. (2024). The historical impact of climate change on the economy was moderate. Thus, we first calibrate the economic part of our model by disregarding climate damages (business as usual or BAU). We then discuss the climate parts. The resulting market-based calibration is summarised in Table 1. Section 6.2 considers ethics-based calibrations with a lower discount rate to capture that policymakers may be more patient than the market.

5.1 *Macroeconomic uncertainties*

For the normal macroeconomic uncertainty, we assume an annualised standard deviation of capital growth of 2% ($\sigma = 2\%/\text{year}^{1/2}$), matching the historical volatility of consumption growth (cf. Wachter, 2013). For the recurring macroeconomic and climate-related disasters, we assume that the recovery rates, $Z_i = 1 - \ell_i$, $i \in \{e, c\}$, have power distributions over $(0, 1)$ with parameters $\beta_i > 0$. The jump size distribution is thus determined by the density function $\zeta_i(Z_i) = \beta_i Z_i^{\beta_i - 1}$, $Z_i \in (0, 1)$ (cf. Pindyck and Wang 2013), so that the n^{th} moment of the recovery rate is $\mathbb{E}[Z_i^n] = \frac{\beta_i}{\beta_i + n}$. We follow Barro and Jin (2011) and define a disaster as an event that destroys more than $\ell_e^\star = 10\%$ of the capital stock, GDP and aggregate consumption. With this cut-off, their historical consumption data suggest an annual disaster probability of 3.8% and average loss of 20% when a disaster strikes, i.e., $\mathbb{E}[\ell_e | \ell_e > \ell_e^\star] = 0.2$ and $\lambda_e \int_0^{1-\ell_e^\star} \zeta_e(Z_e) \mathrm{d}Z_e = 3.8\%$/year. These values give the coefficients $\beta_e = 8$ and $\lambda_e = 8.8\%$/year.

5.2 *Preferences and production*

We follow van den Bremer and van der Ploeg (2021) and use an energy share of $1 - \alpha = 4.3\%$ and an energy cost parameter of $b = \$540$ per ton of carbon. Given an initial world GDP of $Y^{(0)} = \$115$ trillion/year, this corresponds in a BAU scenario with $P = 0$ to an initial fossil use of $F_0 = 115 \times 0.043/0.54 = 9.16$ GtC/year (giga tons of carbon per year). We set intergenerational inequality aversion to $\eta = 1.5$ corresponding to an elasticity of intertemporal substitution of 2/3, close to the value in the DICE model. There is an ongoing debate in the asset pricing literature on this parameter. E.g., Vissing-Jørgensen and Attanasio (2003), combine equity and consumption data and estimate an EIS $(1/\gamma)$ of 1.5. On the other hand, Hall (1988) estimates an EIS well below one.

Given these parameter choices, we calibrate the remaining parameters to match expected GDP growth $g^{(0)} = 2\%$ per year in normal times, so that without rare macroeconomic disasters we have an average consumption rate of $\frac{C^{(0)}}{B^{(0)} K} = 73\%$ of GDP, a risk-free interest rate of $r_f = 0.8\%$/year, an equity premium of 6.5%/year, an expected return on risky assets of 7.3%/year, and a Tobin's Q of $q^{(0)} = 1.38$ (cf. Pindyck and Wang, 2013; Hambel et al., 2021a). They imply that the growth- and risk-adjusted discount rate needed to calculate the SCC is $r^\star = 5.3\%$/year. Without climate change (as used for the zeroth-order approximation), we can obtain closed-form expressions for these quantities (see Appendix B) to pin down the remaining preference and production parameters: $\rho = 5.08\%$/year, $\gamma = 5.347$, $A^* = 0.1231$, and $\varphi = 12.5$ (see Table 1).

TABLE 1. Market-Based Calibration.

Preferences	Coefficient of relative risk aversion: $\gamma = 5.347$ Coefficient of intergenerational inequality aversion: $\eta = 1.5$ Elasticity of intertemporal substitution: $1/\eta = 0.6667$ Pure rate of time preference: $\rho = 5.08\%$/year
Economy	Initial world GDP (2021): $Y_0^{(0)} = \$115$ trillion/year Initial world capital stock (2021): $K_0 = \$1150$ trillion Total factor productivity: $A^* = 0.1231$ and $B(0,0) = 0.1$ Adjustment cost parameter: $\varphi = 12.5$ year
Macroeconomic uncertainties	*Capital stock:* Growth in normal times: $\overline{g}^{(0)} = 2\%$/year Standard deviation of capital growth: $\sigma = 2\%$/year$^{1/2}$ *Macroeconomic disasters (not climate related):* Arrival rate of disasters: $\lambda^e = 8.8\%$/year Mean size of disasters: $\mathbb{E}[\ell_e] = 20\%$ Shape parameter of power distribution: $\beta^e = 8$ *Macroeconomic disasters (climate related):* Mean size of disasters: $\mathbb{E}[1 - Z^c] = 1.58\%$ Shape parameter of power distribution: $\beta^c = 62.29$ Arrival rate of disasters: $\lambda_{0T}^c = 0.06\%$/year and $\lambda_{1T}^c = 9.15\%$/year/°C
Fossil fuel	Initial global emissions in BAU scenario (2021): $F_0 = 9.157$ GtC/year Share of fossil fuel in value added: $1 - \alpha = 4.3\%$ Cost of fossil fuel: $b = 540$ \$/tC
Temperature	Transient climate response to cumulative emissions (pre-tip): $\chi_{\text{pre}} = 1.8$°C/TtC Initial cumulative emissions and temperature (2021): $E_0 = 611.11$ GtC, $T_0 = 1.1$°C Damage function: $D_{1T} = 1.31\%$/°C, $D_{0T} = -0.77\%$
Climate tipping point	Marginal arrival rate of (first) tipping point: $h_{1T} = 0.35\%$/°C/year Tipping threshold: $T^* = 1$°C Arrival rate of subsequent tipping: $h_{2T} = 8\%$/year Number of tipping states: $\overline{H} = 6$ Transient climate response to cumulative emissions (post-tip): χ_{post} =2.4°C/TtC

5.3 *Climate system and global warming damages*

Initial temperature Cumulative emissions since the beginning of the industrial revolution are 611.1 GtC, which given $\chi = 1.8$°C/TtC corresponds to $T_0 = 1.1$°C, both in 2021, well in line with data from NOAA and NASA.[23]

Damages to output Howard and Sterner (2025) perform a meta study of global warming damages and arrive at the preferred damage function $D = 0.00622T^{1.5}$ *excluding* catastrophic events and growth rate effects, implying non-catastrophic level impacts of 3.2% of GDP for global average surface temperature increases of 3°C, far exceeding the

[23]NOAA reported that the 2021 global land and ocean temperature was 1.04°C above the pre-industrial average, see https://www.ncei.noaa.gov/news/global-climate-202112. NASA reports that Earth in 2021 was about 1.1°C hotter than in late 19th century, see https://science.nasa.gov/earth/earth-observatory/2021-continued-earths-warming-trend-149321/.

non-catastrophic level impact in the meta analyses of Nordhaus and Moffat (2017), Barrage and Nordhaus (2024), and Tol (2024). We calibrate our damage function to fit the non-catastrophic damage function of Howard and Sterner (2025) in the range of 1°C to 3°C, giving $D_{0T} = -0.77\%$ and $D_{1T} = 1.31\%/°\text{C}$, which is a very good approximation (see Figure C.1 in Appendix C).

Climate-related disasters For the calibration of temperature-related risk of climate-related disasters, we follow Karydas and Xepapadeas (2022). Those authors use data from the International Disaster Database EM-DAT, split their sample into ten decades, and calculate the disaster intensity for each decade. They find that the climate-related disaster intensity rises almost linearly with temperature from 1960 onwards (see Figure C.2 in Appendix C). They estimate $\lambda_0^c = 0.06\%$/year and $\lambda_{1T}^c = 9.15\%$/year/°C as well as an expected loss of 1.58% and thus $\mathbb{E}[1 - Z_c] = 0.0158$.[24] We fit a power distribution to this expected loss and obtain $\beta_c = 62.29$. Climate-related disasters occur more frequently than non-climate-related macroeconomics disasters,[25] but tend to have a much smaller negative impact on the economy when they strike. To put those numbers in perspective, an initial temperature anomaly of $T_0 = 1.1°\text{C}$ in 2021 implies that the initial one-year probability of a climate disaster with an average damage of 1.58% of output ($1.817 trillion) is $1 - \mathrm{e}^{-0.0006 - 0.0915\,T_0} \approx 9.63\%$. The expected annual loss of output which can be attributed to climate disasters is thus $9.63\% \times 1.58\% \times \$115$ trillion $= \$175$ billion per year, which is in line with the figures reported in UN (2020).[26]

Cascading climate tipping points As Cai and Lontzek (2019) among others point out, the calibration of climate tipping points is highly speculative, since precise knowledge of these events is not available, as those events have not occurred yet. The calibration of the arrival rate of climate tipping in Cai and Lontzek (2019) relies on elicitation of expert views (e.g., Kriegler et al., 2009). We follow their calibration and consider a directed Markov chain with one pre-tipping state, four intermediate states, and one post-tipping state. These intermediate states must be passed through one after the other to reach the post-tipping state, so that tipping cannot be stopped once it has begun.

We follow Cai and Lontzek (2019) and use their benchmark calibration. More precisely, we assume that (i) tipping is only possible if the temperature exceeds $T^* = 1°\text{C}$, and the marginal hazard rate of climate tipping is $h_{1T} = 0.0035$, (ii) it takes an average of 50 years to reach the post-tipping state leading to $h_{2T} = 0.08$, (iii) the impact of climate

[24] Appendix C discusses a calibration where the disaster intensity rises exponentially with temperature.

[25] E.g., at 2 degrees Celsius $\lambda_c = \lambda_{T0}^c + \lambda_{T1}^c T = 19.5\%$/year > $\lambda_e = 8.8\%$/year. This is true for all $T > 0.89°\text{C}$.

[26] UN (2020) reports that extreme major weather events have roughly doubled from 1980-1999 to 2000-2019 (from 4,212 to 7,348 events) with a global economic cost of $1.63 and $2.97 trillion, respectively. Focusing at the period 2000-2019, we estimate the aggregate GDP loss by the following back-on-the-envelope calculation: taking 2010 GDP and temperature and multiplying the result by 20, we obtain an approximate aggregate loss of $20 \times (1 - \mathrm{e}^{-0.0006 - 0.0915 \times 0.95}) \times 1.58\% \times \$93$ trillion $= \$2.45$ trillion over this period, where 0.95°C is the temperature increase in 2010. This is in the ballpark of the reported UN figures. For further and more detailed discussion on the evidence of global warming on the frequency of climate-related events (river floods, tropical cyclones, crop failure, wildfires, droughts, and heatwaves), see Lange et al. (2020).

tipping increases linearly with each new tipping state. Therefore, the transition intensity for climate tipping in the pre-tipping state is $h(E,1) = 0.0035\max(\chi_{\text{pre}}E - 1, 0)$.[27] To model the impact of climate tipping on temperature, we assume a gradual linear increase of the TCRE from $\chi_{\text{pre}} = 1.8°\text{C/TtC}$ to $\chi_{\text{post}} = 2.4°\text{C/TtC}$, i.e., $\chi(H) = \chi_{\text{pre}} + \frac{H-1}{\bar{H}-1}(\chi_{\text{post}} - \chi_{\text{pre}})$. These values are within the ranges reported in Allen et al. (2009) and Matthews et al. (2009).

5.4 *Small parameters*

We can now use the foregoing calibration to evaluate whether the parameters we set to be small in Section 3.1 are indeed small (i.e., $\ll 1$). We obtain $\hat{D}_1 = D_{1T}\chi_{\text{pre}}F_0/(g_0(1 - D_0)) = 0.011 \ll 1$ and $\hat{\lambda}_1^c = (\lambda_{1T}^c\chi_{\text{pre}}F_0\mathbb{E}[\ell_c])/(g_0^2) = 0.060 \ll 1$, making the approximations made to obtain Result 1 likely valid with expected (relative) errors of the order between $\mathcal{O}((7.5\times10^{-3})^2) = \mathcal{O}(6\times10^{-5})$ and $\mathcal{O}(0.060^2) = \mathcal{O}(4\times10^{-3})$. The parameters that govern the pre-tipping hazard rate of tipping, $\hat{h}_{0,\text{pre}} = h_{1T}(T_0 - T^*)/g_0 = 0.018 \ll 1$, and its dependence on temperature, $\hat{h}_1 = h_{1T}\chi_{\text{pre}}F_0/g_0^2 = 0.14$, are also small, although the latter assumption is likely to result in a larger but acceptable error. Finally, the tipping rate of subsequent tips $\hat{h}_{0,\text{post}} = h_{2T}/g_0 = 4.0 = \mathcal{O}(1)$ is not small, making Result 2 likely invalid once tipping has started. In practice, this effect will be mitigated due to the smallness of $\hat{h}_{0,\text{pre}}$ and $\hat{h}_1$, making Result 2 likely a reasonable approximation before the first tip occurs.

6. How Accurate is the Rule for the Optimal SCC?

To test the accuracy of our rules for the optimal SCC in Results 1 and 2, we use the market-based calibration in Table 1 as well as two ethics-based calibrations with lower discount rates. We use our rules to calculate an estimate of the optimal SCC and compare this with the optimal SCC obtained from full numerical optimisation of the model based on a grid-based finite-difference approach (cf. Munk and Sørensen (2010) and see Appendix F).[28] Further tests on the accuracy of our rule can be found in Appendix E.[29]

[27] Notice that Cai and Lontzek (2019) report transition probabilities rather than transition intensities. Our calibration results when the exponential structure of probabilities in Cai and Lontzek (2019) is converted into transition intensities or hazard rates. A hazard rate of $h(E,1) = h_{1T}\max(\chi_{\text{pre}}E - 1, 0)$ translates into an approximate one-year tipping probability of $p_{tip,t} \approx 1 - \mathrm{e}^{-h_{1T}\max(\chi_{\text{pre}}E_t - 1, 0)}$.

[28] In Appendix F, we show that by eliminating K, the problem can be reduced to a numerical optimisation problem in a single state variable, E, and time. We solve this using 4 time steps per year and 100 nodes for E. More time steps or a finer grid do not increase the accuracy of the numerical results, and we can conclude the numerical solutions have converged.

[29] We stress that a simple back-of-the envelope rule does not work, except perhaps for the contributions of internalising damages to productivity to the SCC (but even then, one needs to know the discount rate that includes precautionary savings terms). Since climate disasters destroy the capital stock, the costs of reconstruction (via Tobin's Q) must be taken into account. Further, the disaster damage has a nonlinear effect on welfare due to the correction for risk aversion. Ignoring these effects may underestimate the contribution of disaster risk to the SCC, especially if the discount rate is small.

TABLE 2. Calculation of the Optimal SCC (\$/tCO_2) using the Market-Based Calibration.

(a) Without gradual climate tipping

Externalities	Rule (\$/tCO_2)	Numerical (\$/tCO_2)	Error	$r^\star$ (%/year)
TFP damages only	13.92	13.94	–0.08%	5.30%
Climate disasters only	23.91	23.95	–0.18%	5.24%
TFP damages and climate disasters	37.96	38.05	–0.24%	5.23%

(b) With gradual climate tipping

Externalities	Rule (\$/tCO_2)	Numerical (\$/tCO_2)	Error	$r^\star$ (%/year)
TFP damages only	14.31	14.23	0.59%	5.30%
Climate disasters only	24.60	24.47	0.52%	5.24%
TFP damages and climate disasters	39.11	38.86	0.64%	5.23%

Note: Results are based on the calibration summarised in Table 1 and compare the performance of the rule to the numerical solution. The last column shows how the three climate externalities affect the growth- and risk-adjusted discount rate $r^\star$, compared to 5.30%/year with no climate change.

6.1 *Magnitude of the optimal SCC*

Using the market-based calibration Table summarises the results for six different settings using the market-based calibration in Table 1. Panel (a) indicates that the accuracy of the simple rule in Result 1 for models without a climate tipping point is excellent; the deviation between our estimate of the optimal SCC from our simple rule and the numerical solution is always less than 0.25%. Panel (b) shows that the error is slightly higher if the rule also takes account of the temperature-related risk of climate tipping, but still less than 0.65% and negligible for practical purposes. The risk of climate tipping calls for a slightly higher carbon price, in line with the detailed analysis of Dietz et al. (2021a), who find that, collectively, climate tipping points increase the SCC by about a quarter (our effect is smaller as we have only one type of climate tipping).

We can draw several quantitative conclusions. First, values of the optimal SCC are relatively small, which is due to the relatively high discount rates that follow from the market-based calibration (see values of $r^\star$ in Table). Second, climate disasters are the dominating driver of the optimal SCC and they contribute more than twice as much as TFP damages. Third, compared to climate-related disaster risk, climate tipping risk contributes relatively little to the SCC. In the full-fledged model with all three negative externalities, the optimal SCC is \$39/tCO_2. Most of this is due to climate-related risks and very little is due to gradual climate tipping (see also Table 3(a)). Hence, ignoring climate disaster risks leads to a significant underestimate of the SCC, and thus the need to extend the analysis of van den Bremer and van der Ploeg (2021) to allow for such risks.

The final columns of Table indicate that the growth- and risk-adjusted discount rate, $r^\star$, falls, especially due to recurring climate-related disasters. This is due to precautionary savings, and it further boosts the increase in the optimal SCC. We also compare $r^\star$ with its numerical optimum and find that it approximates the true value reasonably well

TABLE 3. Ethics-Based Calculation of Optimal SCC (US \$/tCO_2) with Lower Discount Rates.

(a) Market-based calibration with $r^\star = 5.3\%$/year

Externalities	Rule (\$/tCO_2)	Share of SCC	Numerical (\$/tCO_2)	Share of SCC	Relative Error
TFP damages only	13.92	35.6%	13.94	35.9%	–0.14%
+ climate disasters	24.04	61.5%	24.11	62.0%	–0.29%
+ climate tipping	1.15	2.9%	0.81	2.1%	41.98%
Total	39.11	100.0%	38.86	100.0%	0.64%

(b) Ethics-based calibration with $r^\star = 3\%$/year

Externalities	Rule (\$/tCO_2)	Share of SCC	Numerical (\$/tCO_2)	Share of SCC	Relative Error
TFP damages only	24.67	27.5%	24.77	27.4%	–0.40%
+ climate disasters	60.03	66.9%	61.07	67.4%	–1.70%
+ climate tipping	4.97	5.5%	4.71	5.2%	5.52%
Total	89.67	100.0%	90.55	100.0%	–0.97%

(c) Ethics-based calibration with $r^\star = 2\%$/year

Externalities	Rule (\$/tCO_2)	Share of SCC	Numerical (\$/tCO_2)	Share of SCC	Relative Error
TFP damages only	36.93	22.0%	37.25	21.6%	–0.86%
+ climate disasters	116.30	69.2%	119.94	69.6%	–3.03%
+ climate tipping	14.94	8.9%	15.22	8.8 %	–1.84%
Total	168.17	100.0%	172.41	100.0%	–2.46%

Note: Apart from the lower choice of utility discount rates ρ in panels (b) and (c) (i.e., $\rho = 2.27\%$ and 1.06%, respectively, instead of 5.08% per year), to ensure that $r^\star$ equals 3%/year and 2%/year, respectively, results are based on the calibration summarised in Table 1.

in all specifications. The difference at the start of the simulation is a maximum of two basis points, with the difference increasing over time.

Using the ethics-based calibration Our market-based calibration matches the equity premium r_p in (25), the return on safe assets r_f in (26), the return on risky assets $r_f + r_p$, and the economic growth rate. This leads to the discount rate (23), needed for our estimate of the optimal SCC from Result 1 or 2. However, our calibration has a rather high pure rate of time preference of $\rho = 5.08\%$/year. In contrast, Stern et al. (2006) follow Frank Ramsey and argue that discounting the utility of future generations is unethical and thus an almost zero pure rate of time preference should be used.

Here, we thus analyse the effects on the optimal SCC if we use a lower utility discount rate of $\rho = 2.27\%$/year, corresponding to $r^\star = 3\%$/year, or an even lower utility discount rate of $\rho = 1.06\%$/year, corresponding to $r^\star = 2\%$/year, instead of the market-based $\rho = 5.08\%$/year given in Table 1 and the corresponding $r^\star = 5.3\%$/year. These ethics-based discounting choices assume that policy makers are more patient than the private sector.[30]

Table 3 reports our estimates of the optimal SCC for these two lower as well as the higher market-based discount rates. We observe the following. Our rule for the SCC, if we allow for all three global warming externalities, gives a SCC of \$90/tCO_2 if $r^\star = 3\%$/year and \$168/tCO_2 if $r^\star = 2\%$/year, much higher than the SCC with market-based interest rates. Rennert et al. (2022) uses a near-term risk-free discount rate of 2%/year and also allows for various types of climate risk. They obtain a SCC of \$185/tCO_2, which would be lower if they had used a growth-corrected $r^\star$ of 2%/year. Barrage and Nordhaus (2024) uses lower damages, a higher market-based discount rate, and obtain a much lower estimate of the SCC. Bilal and Kaenzig (2026) find a SCC a factor about 6 higher than our \$168/tCO_2 and that of Rennert et al. (2022). Moore et al. (2024) obtain a synthesis of 1,823 estimates of the SCC from 147 studies. This gives a relatively high SCC due to structural model variation and uncertainties, because the distribution of published 2020 SCC values is wide and substantially right-skewed (with a lower truncated mean of \$132/tCO2). Golosov et al. (2014) use a time preference rate of 1.5%/year, which given logarithmic utility, implies a discount rate of $r^\star = 1.5\%$ and an optimal SCC of \$15.5/tCO_2, significantly lower than our estimate if we include all three externalities (despite using a low value of the discount rate). Note that, with a risk- and growth-adjusted discount rate of $r^\star = 1.5\%$ (instead of 5.3%), our rule gives \$49.2/tCO_2 if we focus on TFP damages only, which is still a bit more than three times the Golosov et al. (2014) estimate of the optimal SCC. The reason is that our damages are based on Howard and Sterner (2025), which gives much higher damages than those in Golosov et al. (2014). Further, the rule of Golosov et al. (2014) drastically underestimates the optimal SCC by ignoring climate-related disasters and climate tipping points. The rules of Hambel et al. (2021b) and Traeger (2023) also ignore climate disasters and climate tipping points.

With the lower discount rates, Table 3 indicates that the effect of recurring climate disasters is even more substantial compared to the effect of the climate tipping point. Unsurprisingly, the numerical errors increase for lower discount rates. Absolute errors of using the rules are at most 1.0% or 2.5% compared to the numerical optimum.

Although the *absolute* contribution (in \$/tCO_2) of all three externalities is inversely linked to the discount rate, the *relative* importance of each component (in %) may shift. Table 3 indicates that for the ethical (market-based) discount rate of 2% (5.3%) per year, the contribution of TFP damages to the SCC is 21.6% (35.9%), the contribution of the risk of recurring climate disasters to the SCC is 69.6% (62.0%), and the contribution of the risk of climate tipping is 8.8% (2.1%). The relative contribution of the risk of climate tipping to the SCC is thus higher while that of TFP damages is lower for lower discount rates. Tipping risk is fundamentally different from TFP damages: while TFP damages hit every generation, tipping comes with a long delay that hits future generations only and harder. This explains why TFP damages account for a smaller share of SCC at low discount rates even though all components contribute more in absolute terms. Therefore, tipping risk should not be neglected, especially if the discount rate is low.

[30] Barrage (2018) shows that the government then needs two instruments to achieve the first-best outcome: a carbon tax to correct for the global warming externalities and a capital subsidy to correct for private-agent savings being sub-optimally low. See also van der Ploeg and Rezai (2022).

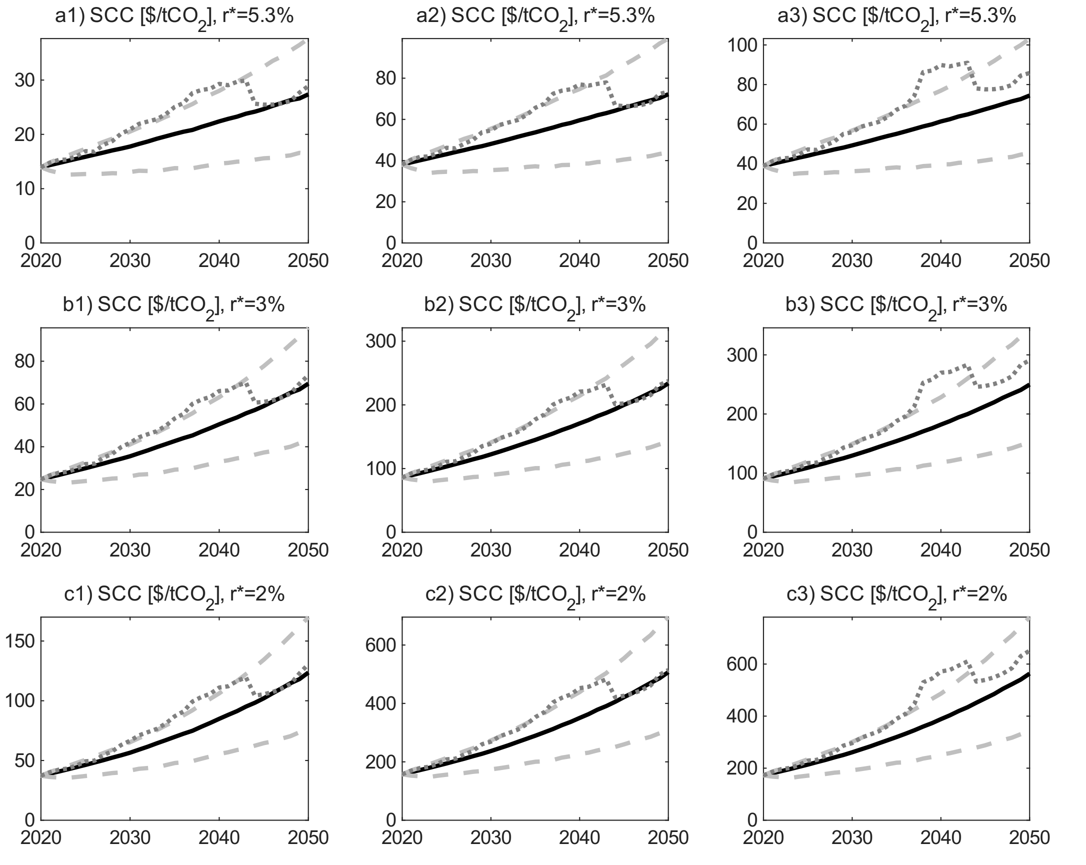

FIGURE 2. Time Series Simulation of the Optimal SCC. Column a) refers to the market-based calibration. Columns b) and c) refer to the ethics-based choices of utility discount rates. Row 1 considers the case with TFP damages only, row 2 considers TFP damages and recurring climate disasters, and row 3 considers all three externalities. The black lines depict the median evolution of the optimal SCC, the dashed lines give 5% and 95% quantiles, and the dotted lines give a sample path.

Finally, the error in using the rule rather than full optimisation to estimate the SCC is higher if the discount rate is low. Not surprisingly, the relative error is slightly higher for the climate tipping component (see Section 5.4), notably for the market-based calibration, albeit this hardly affects the estimate of the SCC (a few cents) as the tipping component is very small if $r^{\star} = 5.3\%$/year and tipping takes a long time (50 years on average once it has begun). For smaller discount rates, the relative error of the climate tipping component decreases significantly, especially if discount rates are low.

6.2 *Scenario Analysis*

To analyse the effects of the three types of global warming externalities and the risk-adjusted discount rate $r^{\star}$ on the optimal SCC over time, Figure 2 plots the evolution of the optimal SCC in nine scenarios. Whenever we vary $r^{\star}$ in this figure, we adjust ρ to

TABLE 4. Road-Testing the Rule for the Optimal SCC (US $/t$CO_2$) in Different Environments.

(a) Market-based calibration with $r^\star = 5.3\%$/year

Model	Rule ($/t$CO_2$)	Numerical ($/t$CO_2$)	Relative Error
Benchmark Model	39.11	38.86	0.64%
Technical progress in fossil-fuel extraction	39.11	38.70	1.06%
Two-sector model	39.11	39.45	–0.86%
Exponential disaster intensity	46.23	46.67	–0.94%
Stochastic climate system	39.11	38.86	0.64%
More general climate tipping model	39.03	38.80	0.59%

(b) Ethics-based calibration with $r^\star = 2\%$/year

Model	Rule ($/t$CO_2$)	Numerical ($/t$CO_2$)	Relative Error
Benchmark Model	168.17	172.41	–2.46%
Technical progress in fossil-fuel extraction	168.17	176.38	–4.65%
Two-sector model	168.17	158.17	6.32%
Exponential disaster intensity	207.59	218.73	–5.09%
Stochastic climate system	168.17	172.75	–2.65%
More general climate tipping model	165.46	170.19	–2.78%

Note: The rule for the optimal SCC is tested outside the realm for which it was derived.

always match the same risk-free rate and risk premium. The three columns refer to the three different values of $r^\star$, and the three rows to the three types of climate externalities. In the first row, there are only damages to TFP, in the second row there is also the risk of recurring climate-related disasters, and the last row shows the SCC with all three types of externalities. The black lines depict the median evolution of the SCC in the respective scenario, the dashed lines the 5% and 95% quantiles, and the dotted lines show a particular sample path.[31] Comparing the first and the second columns, it is apparent that recurring climate disasters give the SCC a boost. In contrast, the tipping point provides a relatively small additional contribution to the median evolution of the SCC. However, if the tipping risk materialises in a particular path, as shown in the dotted lines , the SCC experiences a significant jump upward of about 20%. The result holds regardless of the discount rate, but the SCC decreases sharply in $r^\star$. It is also shown that for lower discount rates, the 5% quantile of SCC increases faster than in the market-based calibration with the higher utility discount rate.

7. Road-Testing the SCC Rule in Different Models

Supply side We conjecture that our rule might also perform well in AK-style models with a different supply side. To test this, we conduct two more tests of the robustness of our rule by checking how well it performs compared to the true numerical optimum

[31] All paths are simulated using the same random numbers in all nine scenarios.

in models with a different supply side than we have assumed: (1) technical progress in the production of fossil fuel (with the cost dropping by 2% per year due to technical progress) and (2) the economy has two sectors, a green and a carbon-intensive one (see for further details Hambel et al. (2024) for technical details).[32] Neither of these alterations of our economic model affects our rule for the optimal SCC except through its effects on aggregate economic activity (see Appendix H). Rows 2 of the two panels in Table indicate that the rule still gives a good approximation to the numerical optimum, slightly less with an ethical discount rate of 2%/year.[33] The reason is that the optimal value of the SCC itself is not much affected by technological progress in fossil fuel production.

We also tested whether our rule for the SCC works well in a neoclassical Solow-Swan growth and climate model with sluggish recovery of the capital stock for the benchmark calibration with $r^{\star}$=5.3%/year (see Appendix G). Although the first component of Rule 2 related to productivity damages works well if the economy is close to the steady state, the rule for the optimal SCC does not work well with disaster or climate tipping risk. A comprehensive discussion of the reasons why the rule does not work well when applied to such a model can be found in Appendix H. Hence, in general, one cannot say that the rule is independent of the supply side of the economy. However, the contributions of TFP damages, climate disasters, and climate tipping to the optimal SCC in the numerical optimum are qualitatively not that different (49%, 38%, and 13%, respectively).

Climate side Table also presents three robustness checks for the climate part. The first one assumes that the climate-related disaster intensity increases exponentially with temperature, e.g., Davariashtiyani et al. (2023), Russo and Domeisen (2023).[34] We find that an exponential disaster intensity boosts the SCC somewhat, and the errors increase a bit but stay in a reasonable range (e.g., -0.94% for the market-based calibration). Accuracy of the rule remains relatively high (see also Table in Appendix H).[35]

The second one allows for stochastic temperature dynamics. We follow Hambel et al. (2021a), Barnett et al. (2021), Barnett (2023), among others, and equip our climate model (4) with normally-distributed temperature shocks. These take account of unpredictable deviations in the relationship between temperature and cumulative emissions (see Appendix D). Table (see also Table in Appendix H) shows that normally-distributed shocks

[32]This two-sector model also allows for damages to aggregate output, risks of climate-related disasters, and a climate tipping point, and assumes that the two consumption goods produced are perfect substitutes and that reallocation of capital from the dirty to the green capital stock is costly. Computationally, it is significantly more complex due to an extra state variable. Our simple rule is not affected by this issue.

[33]We have also tested the rule for the optimal SCC in 2-sector settings with imperfect substitution between clean and carbon-intensive final goods (using a CES-consumption bundle). The results indicate that this has a negligible influence on the optimal SCC.

[34]We replace the parameter λ_{1T} in (22) by $\frac{\partial \lambda_c}{\lambda T}$ and recalibrate the disaster intensity as $\lambda_c(T) = 1.26\mathrm{e}^{0.0845T} - 1.27\%$/year (see also Appendix C).

[35]The accuracy of our rule for a nonlinear relationship between the hazard rate and temperature could be improved by re-evaluating the first-order solution (even without tipping risk). This would give an additional convexity-correction term to capture future temperature increases and resulting in a slightly increased SCC (see Result 2 and Appendix A.4.2 of van den Bremer and van der Ploeg (2021) for such correction terms for convex damages).

in the temperature dynamics leave the SCC largely unaffected, so that the relative errors of the rule also remain almost equally low. This confirms that our rule also works well in models with stochastic temperature shocks.

Finally, we allow for a more general climate tipping Markov chain, where climate tipping may never occur by adding an extra absorbing climate state to our Markov chain that leaves the TCRE unaffected (see Figure D.1). We adjust our rule to take this into account (see (49) in Appendix D). Our modified rule still works very well. Table and Table in Appendix H indicate that the SCC is slightly lower if tipping might never occur.

8. Concluding Remarks

We have presented an integrated assessment model of climate and the economy with uncertainties ranging from regular (normal) macroeconomic shocks and risks of recurring macroeconomic and climate-related macroeconomic disasters to an irreversible climate tipping point whose arrival rate increases with global warming and whose impact takes time to have its full effect. We have applied perturbation analysis to obtain a tractable and intuitive rule for the optimal SCC that deals with all these uncertainties. The rule internalises the externalities arising from the adverse effects of emissions on production damages, the frequency of temperature-dependent recurring climate disasters and the temperature-dependent risk of a gradual climate tipping point.

Our numerical results indicate that the temperature-related risk of recurring climate disasters matters most; it contributes 62% to the overall SCC. Climate tipping only contributes 2% to the SCC, since its full impact is only felt after considerable time and the discount rate is high in the market-based calibration. Just focusing attention on the adverse effects of global warming can thus be seriously misleading. Also, the SCC is higher with a lower social rate of discount. Using a growth-corrected rate of 2%/year instead of the market-based value of 5.3%/year increases the SCC from \$39/tCO_2 to \$172/tCO_2, with now 70% due to the risk of climate disasters and only 22% due to TFP damages.

Our rule is quite accurate compared to full numerical optimisation, also for the individual components of the SCC. The exception is the error in the tipping component in the market-based calibration, but tipping is then irrelevant (as the discount rate is big and tipping takes a long time) and thus the contribution to the SCC is tiny (only a few cents). The relative importance of the correction for production damages to the SCC is less for lower discount rates, while the contribution of tipping risk is higher as then policy makers care more about the future. Tipping risk is thus fundamentally different from productivity damages: while production damages hit every generation, tipping comes with a substantial delay that hits future generations only.

We have also tested the robustness of our rule in more general models for which the rule was not designed. With ongoing technological progress in the production of fossil fuel or a two-sector growth model (with either imperfect or perfect substitution between the carbon-intensive and green final goods), the rule for the optimal SCC still performs remarkably well. Slight modifications of the rule for the optimal SCC also perform well if the frequency of climate-related disasters increases exponentially in temperature, there are normally distributed shocks to temperature, and there is a chance that the climate system never tips.

Both the accuracy and robustness of our estimates of the SCC are thus good, especially if the parameters that we assume to be small — the sensitivities of the damage ratio and the risk of climate-related disasters with respect to temperature and the risk of climate tipping — are indeed small enough, as they are in our calibration, and the discount rate is not too small. While our analytical rules are formally valid only in the limit in which several small parameters approach zero, in practice, they provide robust estimates of the SCC for a much wider and realistic range of parameter space. If we allowed for higher-order terms in the derivation of the optimal SCC, the accuracy of our rule would improve further. Our rules are 'local' in the sense that they exploit the marginal dependencies of damages and the arrival rate of recurring disaster on temperature being constant.

Future research might examine how rules for the optimal SCC perform in more general settings.[36] One possibility is to allow for *multiple* recurring climate-related disasters, varying from floods, droughts, hurricanes to bush fires. Each of these disasters may have different intensities and distributions. Following Cai et al. (2016) and Lemoine and Traeger (2016b) one can also allow for *multiple* climate tipping points.[37] Further extensions of the rules for the SCC can deal with more general carbon cycle and temperature dynamics, uncertainty in and convexity of the damage ratio, uncertainty in the temperature response, and correlations between the shocks to the climate, damages, and the economic system. They may also deal with nonlinear positive feedback effects in the climate system and with tail risks arising from skewed distributions. These extensions would relax the 'local' nature of our approximations.

AI-based techniques may have an increasing role to play. For example, Friedl et al. (2023) use deep-learning algorithms to derive optimal climate policies under economic, climatic and damage uncertainties, including tipping points and parametric uncertainty. A Gaussian-based surrogate model is estimated and used to analyse the SCC with respect to uncertain model parameters. In future work, symbolic regression may be used to obtain an accurate rule for the optimal SCC.[38] Such developments have the potential to provide a step change in our understanding of carbon pricing in uncertain environments.

[36] See van den Bremer and van der Ploeg (2021) for some such extensions.

[37] Lenton et al. (2008) and Lenton (2021) have identified nine of these; e.g., melting and disintegration of the Antarctic or Greenland Ice Sheet, melting of the permafrost, or breakdown of the Atlantic meridional overturning circulation.

[38] In a different field of application, Haefner et al. (2023) obtain perturbations of wave models to explain rogue waves with large-scale machine learning. They use causal analysis, deep learning, parsimonious model selection, and symbolic regression to obtain a symbolic model (i.e., a 'rule') for oceanic rogue waves consistent with the underlying physical processes, both confirming and extending existing theories.

References

Allen, M. R., D. J. Frame, C. Huntingford, C. D. Jones, J. A. Lowe, M. Meinshausen, and N. Meinshausen (2009), "Warming caused by cumulative carbon emissions towards the trillionth tonne." *Nature*, 458 (7242), 1163–1166. [3, 22]

Bansal, R. and A. Yaron (2004), "Risks for the long run: A potential resolution of asset pricing puzzles." *The Journal of Finance*, 59 (4), 1481–1509. [4, 6]

Barnett, M. (2023), "Climate change and uncertainty: An asset pricing perspective." *Management Science*, 69 (12), 7562–7584. [9, 28]

Barnett, M., W. Brock, and L. P. Hansen (2020), "Pricing uncertainty induced by climate change." *The Review of Financial Studies*, 33 (3), 1024–1066. [6]

Barnett, M., W. Brock, and L. P. Hansen (2021), "Climate change uncertainty spillover in the macroeconomy." *NBER Macroeconomics Annual*, 36. [6, 9, 28]

Barrage, L. (2014), "Supplementary material: Sensitivity analysis for Golosov, Hassler, Krusell, and Tsyvinski (2014): 'Optimal taxes on fossil fuel in general equilibrium'." *Econometrica*, 82 (1), 41–88. [5]

Barrage, L. (2018), "Be careful what you calibrate for: social discounting in general equilibrium." *Journal of Public Economics*, 160, 33–49. [25]

Barrage, L. and W. D. Nordhaus (2024), "Policies, projections, and the social cost of carbon: Results from the DICE-2023 model." *Proceedings of the National Academy of Sciences*, 121, e2312030121. [4, 21, 25, 16, 17]

Barro, R. J. (2006), "Rare disasters and asset markets in the twentieth century." *The Quarterly Journal of Economics*, 121 (3), 823–866. [4]

Barro, R. J. (2009), "Rare disasters, asset prices, and welfare costs." *American Economic Review*, 99 (1), 243–64. [4, 6, 16]

Barro, R. J. and T. Jin (2011), "On the size distribution of macroeconomic disasters." *Econometrica*, 79 (5), 1567–1589. [4, 19]

Bender, C. M. and S. A. Orszag (1999), *Advanced Mathematical Methods for Scientists and Engineers*. Springer. [11]

Bilal, A. and D. Kaenzig (2026), "The macroeconomic impact of climate change: Global vs. local temperature." *Quarterly Journal of Economics*, forthcoming. [25]

Cai, Y., T. M. Lenton, and T. S. Lontzek (2016), "Risk of multiple interacting tipping points should encourage rapid CO_2 emission reduction." *Nature Climate Change*, 6 (5), 520–525. [8, 30]

Cai, Y. and T. S. Lontzek (2019), "The social cost of carbon with economic and climate risks." *Journal of Political Economy*, 127 (6), 2684–2734. [2, 8, 9, 21, 22, 11]

Campbell, J. Y. (1999), "Asset prices, consumption, and the business cycle." In *J.B: Taylor, M. Woodford (eds.) Handbook of Macroeconomics*, volume 1, Elsevier North-Holland. [6]

Cerra, V. and S. W. Saxena (2008), "Growth dynamics: the myth of economic recovery." *American Economic Review*, 98, 439–57. [7]

Davariashtiyani, A., M. Taherkhani, S. Fattahpour, and S. Vitousek (2023), "Exponential increases in high-temperature extremes in north america." *Scientific Reports*, 13, 19177. [28, 7]

Dell, M., B. F. Jones, and B. A. Olken (2009), "Temperature and income: Reconciling new cross-sectional and panel estimates." *American Economic Review*, 99, 198–204. [7]

Dell, M., B. F. Jones, and B. A. Olken (2012), "Temperature shocks and economic growth: Evidence from the last half century." *American Economic Journal: Macroeconomics*, 4, 66–95. [7]

Dietz, S., J. Rising, T. Stoerk, and G. Wagner (2021a), "Economic impacts of tipping points in the climate system." *Proceedings of the National Academy of Sciences*, 118, e2103081118. [23]

Dietz, S., F. van der Ploeg, A. Rezai, and F. Venmans (2021b), "Are economists getting climate dynamics right and does it matter?" *Journal of the Association of Environmental and Resource Economists*, 8, 895–921. [4, 8]

Dietz, S. and F. Venmans (2019), "Cumulative carbon emissions and economic policy: in search of general principles." *Journal of Environmental Economics and Management*, 96, 108–129. [3]

Douenne, T. (2020), "Disaster risks, disaster strikes, and economic growth: The role of preferences." *Review of Economic Dynamics*, 38, 251–272. [7]

Duffie, D. and L. G. Epstein (1992), "Asset pricing with stochastic differential utility." *The Review of Financial Studies*, 5 (3), 411–436. [6, 16]

Epstein, L. G and S. E. Zin (1989), "Substitution, risk aversion, and the temporal behavior of consumption and asset returns: A theoretical framework." *Econometrica*, 937–969. [6]

Fernández-Villaverde, J. and O. Levintal (2018), "Solution methods for models with rare disasters." *Quantitative Economics*, 9 (2), 903–944. [4, 10]

Fouque, J.P., G. Papanicolaou, and K.R. Sircar (2000), *Derivatives in Financial Markets with Stochastic Volatility*. Cambridge University Press. [3]

Friedl, A., F. Kuebler, S. Scheidegger, and T. Usui (2023), "Deep uncertainty quantification: with an application to integrated assessment models." *Working Paper*, University of Lausanne. [30]

Gabaix, X. (2012), " Variable Rare Disasters: An Exactly Solved Framework for Ten Puzzles in Macro-Finance." *The Quarterly Journal of Economics*, 127, 645–700. [4]

Gollier, C. (2018), *Ethical Asset Valuation and the Good Society*. Columbia University Press. [6]

Golosov, M., J. Hassler, P. Krusell, and A. Tsyvinski (2014), "Optimal taxes on fossil fuel in general equilibrium." *Econometrica*, 82 (1), 41–88. [5, 7, 15, 25]

Gourio, F. (2012), "Disaster risk and business cycles." *The American Economic Review*, 102 (6), 2734–2766. [4, 10]

Haefner, D., J. Gemmrich, and M. Jochum (2023), "Machine-guided discovery of a real-world rogue wave model." *Proceedings of the National Academy of Sciences*, 120, e2306275120. [30]

Hall, R. E. (1988), "Intertemporal Substitution in Consumption." *Journal of Political Economy*, 39, 339–347. [6, 19]

Hambel, C., H. Kraft, and E. S. Schwartz (2021a), "Optimal carbon abatement in a stochastic equilibrium model with climate change." *European Economic Review*, 132, 103642. [2, 7, 8, 9, 19, 28]

Hambel, C., H. Kraft, and E. S. Schwartz (2021b), "The social cost of carbon in a non-cooperative world." *Journal of International Economics*, 131, 103490. [5, 25]

Hambel, C., H. Kraft, and F. van der Ploeg (2024), "Asset diversification versus climate action." *International Economic Review,*, 65, 1323–1355. [18, 28, 6, 15]

Hambel, C. and F. van der Ploeg (2025), "Policy transition risk, carbon premiums, and asset prices." *Journal of Monetary Economics*, 152, 103780. [7]

Hansen, L. P. and J. Miao (2018), "Aversion to Ambiguity and Model Misspecification in Dynamic Stochastic Environments." *Proceedings of the National Academy of Sciences*, 115 (37), 9163–9168. [6]

Hansen, L. P. and T. J. Sargent (2007), "Recursive robust estimation and control without commitment." *Journal of Economic Theory*, 136 (1), 1–27. [6]

Howard, P. H. and T. Sterner (2025), "Methodology matters: A careful meta-analysis of climate damages." *Environmental and Resource Economics*, 88, 3289–3327. [20, 21, 25, 7]

Hsiang, S. M. and A. S. Jina (2014), "The causal effect of environmental catastrophe on long-run economic growth: evidence from 6,700 cyclones." *NBER Working Paper*, 20352. [7]

Isoré, M. and U. Szczerbowicz (2017), "Disaster risk and preference shifts in a New Keynesian model." *Journal of Economic Dynamics and Control*, 79, 97–125. [10]

Jensen, S. and C. P. Traeger (2014), "Optimal climate change mitigation under long-term growth uncertainty: Stochastic integrated assessment and analytic findings." *European Economic Review*, 69, 104–125. [2]

Jensen, S. and C. P Traeger (2021), "Pricing climate risk." *CESifo Working Paper 9196*. [18]

Karydas, C. and A. Xepapadeas (2022), "Climate change financial risks: Implications for asset pricing and interest rates." *Journal of Financial Stability*, 63, 101061. [9, 18, 21, 7, 8]

Kevorkian, J. and J. D. Cole (1996), *Multiple Scale and Singular Perturbation Methods*. Springer. [11]

Kriegler, E., J. W. Hall, H. Held, R. Dawson, and H. J. Schellnhuber (2009), "Imprecise probability assessment of tipping points in the climate system." *Proceedings of the National Academy of Sciences*, 106 (13), 5041–5046. [21]

Lange, S., J. Volkholz, T. Geiger, F. Zhao, I. Vega, T. Veldkamp, C. P. O. Reyer, L. Warszawski, V. Huber, J. Jägermeyr, J. Schewe, D. N. Bresch, M. Büchner, J. Chang, P. Ciais, M. Dury, K. Emanuel, C. Folberth, D. Gerten, S. N. Gosling, M. Grillakis, N. Hanasaki, A.-J. Henrot, T. Hickler, Y. Honda, A. Ito, N. Khabarov, A. Koutroulis, W. Liu, C. Müller, K. Nishina, S. Ostberg, H. Müller Schmied, S. I. Seneviratne, T. Stacke, J. Steinkamp, W. Thiery, Y. Wada, S. Willner, H. Yang, M. Yoshikawa, C. Yue, and K. Frieler (2020), "Projecting exposure to extreme climate impact events across six event categories and three spatial scales." *Earth's Future*, 8, e2020EF001616. [21]

Lemoine, D. (2021), "The climate risk premium: how uncertainty affects the social cost of carbon." *Journal of the Association of Environmental and Resource Economists*, 8 (1), 27–57. [5]

Lemoine, D. and C. P. Traeger (2014), "Watch your step: optimal policy in a tipping climate." *American Economic Journal: Economic Policy*, 6 (1), 137–66. [5, 17]

Lemoine, D. and C. P. Traeger (2016a), "Ambiguous tipping points." *Journal of Economic Behavior & Organization*, 132, 5–18. [17]

Lemoine, D. and C. P. Traeger (2016b), "Economics of tipping the climate dominoes." *Nature Climate Change*, 6 (5), 514–519. [2, 30]

Lenton, T. M. (2021), "Tipping points in the climate system." *Weather, Special Issue: COP26,*, 76, 325–326. [30]

Lenton, T. M., H. Held, E. Kriegler, J. W. Hall, W. Lucht, S. Rahmstorf, and H. J. Schellnhuber (2008), "Tipping elements in the Earth's climate system." *Proceedings of the National Academy of Sciences*, 105, 1786–93. [30]

Levintal, O. (2017), "Fifth-order perturbation solution to DSGE models." *Journal of Economic Dynamics and Control*, 80, 1–16. [10]

Levintal, O. (2018), "Taylor projection: A new solution method for dynamic general equilibrium models." *International Economic Review*, 59 (3), 1345–1373. [10]

Matthews, H. D., N. P. Gillett, P. A. Stott, and K. Zickfeld (2009), "The proportionality of global warming to cumulative carbon emissions." *Nature*, 459 (7248), 829–832. [3, 22]

Moore, F. C. and D. B. Diaz (2015), "Temperature impacts on economic growth Warrant Stringent Mitigation Policy." *Nature Climate Change*, 5, 127–131. [7]

Moore, F. C., M. A. Drupp, J. Rising, S. Dietz, I. Rudik, and G. Wagner (2024), "Synthesis of evidence yields high social cost of carbon due to structural model variation and uncertainties." *Working Paper 32544, NBER, Cambridge, Mass.* [25]

Munk, C. and C. Sørensen (2010), "Dynamic asset allocation with stochastic income and interest rates." *Journal of Financial Economics*, 96, 433–462. [22, 15]

Nayfeh, A. H. (2004), *Perturbation Methods*. Wiley. [11]

Nordhaus, W. D. (1991), "To slow or not to slow: The economics of the greenhouse effect." *The Economic Journal*, 101 (407), 920–937. [5]

Nordhaus, W. D. (1992), "The DICE model: Background and structure of a dynamic integrated climate-economy model of the economics of global warming." Technical report, Cowles Foundation for Research in Economics, Yale University. [8]

Nordhaus, W. D. (2007), "A review of the stern review on the economics of climate change." *Journal of Economic Literature*, 45 (3), 686–702. [6]

Nordhaus, W. D. (2017), "Revisiting the social cost of carbon." *Proceedings of the National Academy of Sciences*, 114, 1518–1523. [15]

Nordhaus, W. D. and A. Moffat (2017), "A survey of global impacts of climate change: Replication, survey methods, and a statistical analysis." *NBER Working Paper*, 23646. [21]

Pindyck, R. S. (2012), "Uncertain Outcomes and Climate Change Policy." *Journal of Environmental Economics and Management*, 63, 289–303. [7]

Pindyck, R. S. and N. Wang (2013), "The economic and policy consequences of catastrophes." *American Economic Journal: Economic Policy*, 5 (4), 306–39. [7, 13, 16, 18, 19, 6]

Rennert, K., F. Errickson, B. C. Prest, L. Rennels, R.G. Newell, W. Pizer, C. Kingdon, J. Wingenroth, R. Cooke, B. Parthum, Smith D, K. Cromar, D. Diaz, F.C. Moore, U.K. Müller, R.J. Plevin, A.E. Raftery, H. Ševčíková, H. Sheets, J.H. Stock, T. Tan, M. Watson, T.E. Wong, and D. Anthoff (2022), "Comprehensive evidence implies a higher social cost of CO_2." *Nature*, 610, 687–692. [2, 25]

Rezai, A. and F. van der Ploeg (2016), "Intergenerational inequality aversion, growth, and the role of damages,: Occam's rule for the global carbon tax." *Journal of the Association of Environmental and Resource Economists*, 3 (2), 493–522. [5]

Rudenbusch, G. D. and E. Swanson (2012), "The bond premium in a dsge model with long-run real and nominal risks." *American Economic Journal: Macroeconomics*, 4, 105–43. [4]

Russo, E. and D. I. V. Domeisen (2023), "Increasing intensity of extreme heatwaves: The crucial role of metrics." *Geophysical Research Letters*, 50, e2023GL103540. [28, 7]

Stern, N., S. Peters, V. Bakhshi, A. Bowen, C. Cameron, S. Catovsky, D. Crane, S. Cruickshank, S. Dietz, and N. Edmonson (2006), *Stern Review: The economics of climate change*, volume 30. HM treasury London. [24]

Su, H., C. Ying, and X. Zhu (2022), "Disaster risk matters in the bond market." *Finance Research Letters*, 47, 102764. [4]

Tol, R. S. J. (2024), “A meta-analysis of the total economic impact of climate change.” *Energy Policy*, 185, 113922. [21]

Traeger, C. P. (2023), “ACE—analytic climate economy.” *American Economic Journal: Economic Policy*, 15, 372–406. [5, 25]

Traeger, C. P. (2025), “Uncertainty in the analytic climate economy.” *Working Paper*, University of Oslo. [5]

Tsai, J. and J. A. Wachter (2015), “Disaster risk and its implications for asset pricing.” *Annual Review of Financial Economics*, 7, 219–252. [4]

UN (2020), “Human cost of disasters: An overview of the last 20 years.” *United Nations office for Disaster Risk Reduction,*, Non-Technical Report. [21]

van den Bijgaart, I. M., R. Gerlagh, and M. Liski (2016), “A simple rule for the social cost of carbon.” *Journal of Environmental Economics and Management*, 77, 75–94. [5]

van den Bremer, T. S. and F. van der Ploeg (2021), “The risk-adjusted carbon price.” *American Economic Review*, 111 (9), 2782–2810. [3, 5, 8, 9, 12, 13, 14, 18, 19, 23, 28, 30, 1]

van der Ploeg, F. and A. Rezai (2022), “Optimal carbon pricing in general equilibrium revisited: temperature caps and stranded assets in an extended annual DSGE model.” *Journal of Environmental Economics and Management*, 100, 102522. [5, 25]

Van Dyke, M. (1975), *Perturbation Methods in Fluid Mechanics*. Parabolic Press, Stanford. [11]

Vissing-Jørgensen, A. (2002), “ Limited Asset Market Participation and the Elasticity of Intertemporal Substitution.” *Journal of Political Economy*, 110, 825–853. [6]

Vissing-Jørgensen, A. and O. P. Attanasio (2003), “Stock-market participation, intertemporal substitution, and risk-aversion.” *American Economic Review*, 93 (2), 383–391. [6, 19]

Wachter, J. A. (2013), “Can time-varying risk of rare disasters explain aggregate stock market volatility?” *The Journal of Finance*, 68 (3), 987–1035. [7, 19]

Withagen, C. (2022), “On simple rules for the social cost of carbon.” *Environmental and Resource Economics*, 82, 461–481. [5]

Appendix A: Application of perturbation theory

We identify the small parameters and rank their relative magnitudes (see Section A.1). We do so by deciding on their order in terms of a single small parameter ϵ. Second, we choose the structure of our perturbation expansion, depending on how and where the small parameter ϵ appears in the HJB equation (see Section A.2). Third, we perform the perturbation expansion, and then solve the HJB equation at zeroth order (see Section A.3) and at first order (see Section A.4), respectively.

A.1 *Identification of the small parameters*

By normalising all variables by their typical values, one can make them non-dimensional, which is standard in the physical sciences. This typically reveals one or more non-dimensional numbers (constants that do not vary in the model, e.g., with time), which measure the relative importance of several components of the model (cf. the Reynolds number in fluid mechanics). By normalising variables by their typical values (e.g., their initial values) the non-dimensional variables thus obtained become (at least initially) $\mathcal{O}(1) = \mathcal{O}(\epsilon^0)$, i.e., 'order 1' or 'zeroth order' in the small parameter ϵ (since $\epsilon^0 = 1$).

In van den Bremer and van der Ploeg (2021) (see their Appendix A.2.1) a model similar to the present one is made non-dimensional using (mostly) initial values of the variables, resulting in 16 non-dimensional numbers, of which 15 are assumed to be $\mathcal{O}(1)$, so their effects are included without approximation, and 1 is set as $\mathcal{O}(\epsilon)$ and included through a perturbation expansion, relying on the relative effect represented by this non-dimensional number being small. This latter number corresponds to the damage ratio, which is typically much smaller than 1.

Non-dimensionalisation We rewrite the HJB equation (8) in non-dimensional form, ensuring the non-dimensional variables thus obtained are $\mathcal{O}(1)$, at least initially, that is, on $\mathcal{O}(1)$ non-dimensional time scales. To do so, we normalise the capital stock K_t and the climate sensitivity χ by their initial values (at $t = 0$). We define non-dimensional time by multiplying by $g_0 = g(E_0)$ in the absence of any further climate change (or tipping). We define the non-dimensional variables $\hat{C} = C/C_0$, $\hat{F} = F/F_0$ and $\hat{K} = K/K_0$, where hats denote non-dimensional variables. Note $F_0 = A_0^{1/\alpha}((1-\alpha)/b)^{1/\alpha} K_0$ with $A_0 = A(E_0)$ is the known initial value of fossil fuel consumption in the absence of any further climate change (and thus assuming a zero carbon price), and $C_0 = g_0 K_0$, since these initial values are not known at this stage in the solution procedure. We make E non-dimensional by $\hat{E} = E/(F_0/g_0)$.[39] Finally, we set $\hat{\chi} = \chi/\chi_{\text{pre}}$, where the initial value of the climate sensitivity is its pre-tipping value χ_{pre}. The third state variable H is already non-dimensional. We can now use this to write the HJB equation (8) in non-dimensional form,

$$0 = \max_{\hat{C},\hat{F}} \Big[\hat{f}(\hat{C}, \hat{J}) + \hat{J}_{\hat{K}} \Big[\hat{A}(\hat{E}, H) \hat{K}^{\alpha} \hat{F}^{1-\alpha} - \hat{C} - \hat{b}\hat{F} - \hat{\delta}\hat{K} - \frac{1}{2}\hat{\varphi}\frac{\hat{I}^2}{\hat{K}} \Big] + \frac{1}{2}\hat{J}_{\hat{K}\hat{K}}\hat{K}^2\hat{\sigma}^2$$

[39] Alternatively, one could define $\hat{E} = E/E_0$, but the convention used has the advantage of characterising future emissions on $\mathcal{O}(1)$ non-dimensional time scales.

$$+\hat{J}_{\hat{E}}\hat{\varpi}\hat{F}+\hat{\lambda}_e\underbrace{\frac{\mathbb{E}\big[\hat{J}\big((1-\ell_e)\hat{K},\hat{E},H\big)-\hat{J}(\hat{K},\hat{E},H)\big]}{\mathbb{E}[\ell_e]}}_{\mathcal{O}(1)} \qquad (29)$$

$$+\hat{\lambda}_c(\hat{E},\hat{H})\underbrace{\frac{\mathbb{E}\big[\hat{J}\big((1-\ell_c)\hat{K},\hat{E},H\big)-\hat{J}(\hat{K},\hat{E},H)\big]}{\mathbb{E}[\ell_c]}}_{\mathcal{O}(1)}+\hat{h}(\hat{E},\hat{H})\big[\hat{J}(\hat{K},\hat{E},H+1)-\hat{J}(\hat{K},\hat{E},H)\big]\Big],$$

where $\hat{J}=J/J_0$, $\hat{f}=g_0f/J_0$, $J_0=C_0^{1-\gamma}/g_0^{\frac{1-\gamma}{1-\eta}}$, $\hat{A}=A/A_0$, $\hat{I}=I/C_0$, $\hat{\lambda}_c=\lambda_c\mathbb{E}[l_c]/g_0$, and $\hat{h}=h/g_0$. Since loss fractions ℓ_e and ℓ_e are typically small, we have absorbed a linear dependence on the expected loss fraction in the non-dimensional hazard rate, so the non-dimensional expected loss of value from recurring disasters, $\mathbb{E}\big[\hat{J}\big((1-\ell_i)\hat{K},\hat{E},H\big)-\hat{J}(\hat{K},\hat{E},H)\big)\big]/\mathbb{E}[\ell_i]$ is $\mathcal{O}(1)$ for $i=e,c$ w.l.g. (provided $\mathbb{E}[1-\ell_i]=\mathcal{O}(1)$ (not small) for $i=e,c$, which is always satisfied). The dependence on climate is captured by

$$\hat{A}=1-\hat{D}_1\hat{E}\hat{\chi},\qquad \hat{\lambda}_c=\hat{\lambda}_0^c+\hat{\lambda}_1^c\hat{E}\hat{\chi},\qquad \hat{h}=\begin{cases}\hat{h}_{0,\mathrm{pre}}+\hat{h}_1\hat{E} & \text{if } H=1,\\ \hat{h}_{0,\mathrm{post}} & \text{if } H=2,\ldots,\overline{H}-1,\\ 0 & \text{if } H=\overline{H}\le 0.\end{cases} \qquad (30)$$

In equations (29)-(30), the following non-dimensional numbers arise

$$\underbrace{\hat{b}=\frac{bF_0}{g_0K_0},\ \hat{\delta}=\frac{\delta}{g_0},\ \hat{\varphi}=\frac{\varphi}{g_0},\ \hat{\sigma}=\frac{\sigma}{\sqrt{g_0}},\ \hat{\varpi}=\varpi,\ \hat{\lambda_e}=\frac{\lambda_e\mathbb{E}[\ell_e]}{g_0},\ \hat{\lambda}_0^c=\frac{\lambda_0^c\mathbb{E}[\ell_c]}{g_0},}_{\mathcal{O}(1)} \qquad (31)$$

which we set to be $\mathcal{O}(1)$ and thus include without approximation, and

$$\underbrace{\hat{D}_1=\frac{D_{1T}\chi_{\mathrm{pre}}F_0}{g_0(1-D_0)},\qquad \hat{\lambda}_1^c=\frac{\lambda_{1T}^c\chi_{\mathrm{pre}}F_0\mathbb{E}[\ell_c]}{g_0^2},}_{\mathcal{O}(\epsilon)}$$
$$\underbrace{\hat{h}_{0,\mathrm{pre}}=\frac{h_{1T}(T_0-T^*)}{g_0},\qquad \hat{h}_1=\frac{h_{1T}\chi_{\mathrm{pre}}F_0}{g_0^2},\qquad \hat{h}_{0,\mathrm{post}}=\frac{h_{2T}}{g_0},}_{\mathcal{O}(\epsilon)} \qquad (32)$$

which we all set to be $\mathcal{O}(\epsilon)$, that is, we set these parameters to be 'equally small' or 'of the same order of magnitude'. Finally, we assume that $\hat{\chi}$ stays $\mathcal{O}(1)$, that is, the increases in χ that occur at tipping are (cumulatively) of the same order of magnitude as χ_{pre}. In our calibration, $\chi_{\mathrm{pre}}=1.8°$C/TtC and $\chi_{\mathrm{post}}=2.4°$C/TtC, in line with this assumption.

A.2 *Perturbation expansion*

We assume that solutions for the value function, J, and the policy variables, C and F, take the general form (cf. van den Bremer and van der Ploeg, 2021)

$$
\begin{aligned}
J(K,E,H) &= J^{(0)}(K,E,H,\epsilon E) + \epsilon J^{(1)}(K,E,H,\epsilon E) + \mathcal{O}\left(\epsilon^2\right), \\
C(K,E,H) &= C^{(0)}(K,E,H,\epsilon E) + \epsilon C^{(1)}(K,E,H,\epsilon E) + \mathcal{O}\left(\epsilon^2\right), \\
F(K,E,H) &= F^{(0)}(K,E,H,\epsilon E) + \epsilon F^{(1)}(K,E,H,\epsilon E) + \mathcal{O}\left(\epsilon^2\right),
\end{aligned} \tag{33}
$$

where the structure of the solution is based on the underlying HJB equation. Generally, the functional dependences in (33) include both E and ϵE. The latter is referred to as a 'slow' functional dependence on E, as differentiating $J^{(0)}$ with respect to E increases the order in ϵ by 1 (unlike differentiating with respect to K, which leaves the order unchanged). Such 'slow' derivatives that increase the order by ϵ are captured by $\epsilon\mathcal{F}^1$ in the operator $\mathcal{F}$ (cf. (13)). In doing so, we leverage the power of the extensive literature on slow-fast dynamics and differential equations (see van den Bremer and van der Ploeg (2021) for an economic application and Fouque et al. (2000) for finance applications).

A.3 *Zeroth-order solution and proof of Result 1*

The zeroth-order solution takes into account the effects of cumulative emissions on damages and on the risk of climate disasters, but not the effects of (future) variations in this stock (their effects are too 'slow' to play a role at this order) and of climate tipping. The zeroth-order expressions for C, F, and Y follow from (9) and (10),

$$
C^{(0)} = \left(J_K^{(0)}\left(1-\varphi\frac{I^{(0)}}{K}\right)\right)^{-\frac{1}{\eta}}\left((1-\gamma)J^{(0)}\right)^{\frac{1}{\eta}\frac{\eta-\gamma}{1-\gamma}}, \tag{34}
$$

$$
F^{(0)} = \left(\frac{(1-\alpha)A(\epsilon E,H)}{b}\right)^{\frac{1}{\alpha}}K, \tag{35}
$$

$$
Y^{(0)} = B^{(0)}K, \tag{36}
$$

where $B^{(0)} \equiv B\big(\epsilon E,H,P=0\big) = A(\epsilon E,H)^{1/\alpha}\big(\frac{b}{1-\alpha}\big)^{1-1/\alpha}$ is total factor productivity in the absence of a carbon price.

Treating the effects of $D(\epsilon E,H)$ on total factor productivity and of $\lambda_c(\epsilon E,H)$ on the risk of macroeconomic disasters as constant when deriving the zeroth-order solution, we substitute the optimality conditions (34) – (36) into the HJB equation (8) and then seek a solution of the form $J^{(0)} = \frac{1}{1-\gamma}K^{1-\gamma}\psi^{(0)}(\epsilon E,H)$, to obtain a (nonlinear) implicit equation in $\psi^{(0)}$:

$$
\begin{aligned}
0 = \frac{1-\gamma}{1-\eta}\Big(\big(\psi^{(0)}\big)^{\frac{\eta-1}{\eta(1-\gamma)}}\big(1-\varphi i^{(0)}\big)-\rho\Big) + (1-\gamma)g^{(0)} - \frac{1}{2}\gamma(1-\gamma)\sigma^2 \\
+ \lambda_e\mathbb{E}\big[Z_e^{1-\gamma}-1\big] + \lambda_c(\epsilon E,H)\mathbb{E}\big[Z_c^{1-\gamma}-1\big],
\end{aligned} \tag{37}
$$

where $i^{(0)} \equiv i^{(0)}(\psi^{(0)}) = \alpha B^{(0)} - \left(\psi^{(0)}\right)^{\frac{1-1/\eta}{1-\gamma}}$ and $g^{(0)} \equiv g^{(0)}(\psi^{(0)}) = -\delta + \alpha B^{(0)} - \left(\psi^{(0)}\right)^{\frac{1-1/\eta}{1-\gamma}} - \frac{1}{2}\varphi\left(\alpha B^{(0)} - \left(\psi^{(0)}\right)^{\frac{1-1/\eta}{1-\gamma}}\right)^2$. The expression for $g^{(0)}$ is not equal to the expected growth rate (e.g., of the capital stock) owing to the presence of non-zero mean disasters, but equals the expected growth rate in normal times when no disasters occur. The solution for $\psi^{(0)}$ depends on the stock of cumulative emissions through $A(\epsilon E, H)$ and $\lambda_c(\epsilon E, H)$. While we can solve equation (37) numerically for $\psi^{(0)}$, it is convenient to express the solution as

$$\psi^{(0)} = \frac{(r^\star)^{\frac{-\eta(1-\gamma)}{1-\eta}}}{\left(1 - \varphi i^{(0)}\right)^{1-\gamma}}, \tag{38}$$

where the (zeroth-order accurate) discount rate $r^\star$ is given by

$$r^\star = \rho + (\eta - 1)\Big[g^{(0)} - \frac{1}{2}\gamma\sigma^2 - \frac{\lambda_e}{1-\gamma}\mathbb{E}\big[1 - Z_e^{1-\gamma}\big] - \frac{\lambda_c(\epsilon E, H)}{1-\gamma}\mathbb{E}\big[1 - Z_c^{1-\gamma}\big]\Big], \tag{39}$$

and the investment rate $i^{(0)} = I_t^{(0)}/K_t$, which is needed to evaluate $g^{(0)} = i^{(0)} - \delta - \frac{1}{2}\varphi\left(i^{(0)}\right)^2$, follows from the nonlinear implicit equation

$$i^{(0)} + \frac{r^\star}{1 - \varphi i^{(0)}} = \alpha\Big(\frac{b}{1-\alpha}\Big)^{1-\frac{1}{\alpha}} A(\epsilon E, H)^{1/\alpha}, \tag{40}$$

which follows from substituting the solutions for the policy variables (34) and the zeroth-order solution for the value function (38) into the budget constraint, $Y - bF - I - C = 0$. In equations (34)-(40), we have made explicit the origin of the 'slow' functional dependence of the solutions (i.e., $\psi^{(0)}$, $g^{(0)}$, $i^{(0)}$, and $r^\star$) on E, that is, through $A(\epsilon E, H)$ and $\lambda_c(\epsilon E, H)$. Finally, we note that the zeroth-order solution is valid for both the pre- and post-tipping problems (so for any H), as the effect of tipping, which causes the pre- and post-tipping problems to differ, arises at higher order.

Proof of Result 1 We evaluate $P_{\text{R1}} = (-J_E^{(0)}/J_K^{(0)})q^{(0)}$ by differentiating $J^{(0)}$ with respect to K and E, where the latter is evaluated using the chain rule from (38) and (39) and an implicit derivative of (40). Only leading-order terms are retained for consistency. □

A.4 *First-order solution and proof of Result 2*

To derive the first-order value function $J^{(1)}$, we begin by noting from the pre-tip HJB equation (8) that the first-order conditions (9) and (10) are unaffected by the climate-tipping term in the HJB equation (the rightmost term in (8)), because this term does not depend directly on the policy variables C and F.

Furthermore, as a result of the linearity of the dependence of the risk of climate-related recurring disasters λ_c and the damage function D on E, their marginal effects $\mathrm{d}\lambda_c/\mathrm{d}E = \lambda_1^c$ and $\mathrm{d}D/\mathrm{d}E = D_1$ are constant and not a function of E, resulting in $J_E^{(0)}$ (as obtained from (38)) being only a 'slow' function of E. As a result, the first-order 'forcing' term $J_E^{(0)}\varpi F^{(0)}$ does not give rise to a first-order value function that is a 'fast' function of E and thus does not yield an additional contribution to the SCC ($P \propto J_E$). We thus ignore this term.

Inspection of the HJB equation (8) shows that a first-order solution of the form $\epsilon J^{(1)} = \epsilon \frac{1}{1-\gamma} K^{1-\gamma}\psi^{(1)}(E,H)$ can be found recursively for $H = 1,\ldots,\overline{H}-1$. Substitution of the series expansion (33) into the HJB equation (8), in which the optimal solutions for the policy variables have already been substituted in from the first-order conditions (9) and (10), retaining only first-order terms in $h = \mathcal{O}(\epsilon)$, and dividing by $K^{1-\gamma}$ gives

$$
\begin{aligned}
0 =& \tfrac{1}{1-\gamma}\big(\psi(E,H+1) - \psi^{(0)}(E,H)\big) - \tfrac{1}{2}\gamma\sigma^2\psi^{(1)}(E,H) \\
&+ \tfrac{\Delta\lambda}{1-\gamma}\psi^{(1)}(E,H)\Big(i^{(1)}\big(1-\varphi i^{(0)}\big)\psi^{(0)}(E,H) + \big(-\delta + i^{(0)} - \tfrac{1}{2}\varphi\big(i^{(0)}\big)^2\big)\psi^{(1)}(E,H)\Big) \\
&+ \tfrac{1}{1-\eta}\Big[-\tfrac{\gamma-\eta}{1-\gamma}\psi^{(0)}(E,H)^{\frac{\eta-1}{1-\gamma}}\Big[-\rho\psi^{(0)}(E,H)^{\frac{1-\eta}{1-\gamma}} \\
&+ \Big(\big(1-\varphi i^{(0)}\big)^{-1/\eta}\psi^{(0)}(E,H)^{\frac{1-\eta}{(-1+\gamma)\eta}}\Big)^{1-\eta}\Big]\psi^{(1)}(E,H) + \psi^{(0)}(E,H)^{1-\frac{1-\eta}{1-\gamma}} \times \\
&\Big[-\tfrac{1-\eta}{1-\gamma}\rho\psi^{(0)}(E,H)^{\frac{1-\eta}{1-\gamma}-1}\psi^{(1)}(E,H) - \tfrac{1-\eta}{\eta(1-\gamma)}\big(1-\varphi i^{(0)}\big)^{-\frac{1}{\eta}}\psi^{(0)}(E,H)^{\frac{1+\gamma-\eta}{1-\gamma}-\frac{1}{(1-\gamma)\eta}} \times \\
&\Big(\varphi i^{(1)}\psi^{(0)}(E,H)(\gamma-1) + \psi^{(1)}(E,H)(1-\eta)\big(1-\varphi i^{(0)}\big)\Big)\Big]\Big],
\end{aligned}
$$

where $\Delta\lambda$ is a shorthand for $\lambda_e\mathbb{E}[Z_e^{1-\gamma}-1] + \lambda_c(E,H)\mathbb{E}[Z_c^{1-\gamma}-1]$, $\psi(E,H) = \psi^{(0)}(E,H) + \epsilon\psi^{(1)}(E,H)$ if $H < \overline{H}$, and $\psi(E,\overline{H}) = \psi^{(0)}(E,\overline{H})$. This equation still has two unknowns, $\psi^{(1)}$ and $i^{(1)}$, and must be solved together with the budget constraint, $Y - bF - I - C = 0$, at the same order of approximation. Again, using equations (9) and (10) and retaining only the first-order terms in $h = \mathcal{O}(\epsilon)$ yields a second equation relating $\psi^{(1)}$ and $i^{(1)}$,

$$
\begin{aligned}
i^{(1)} =& \frac{\psi^{(0)}(E,H)^{\frac{1-\eta}{(\gamma-1)\eta}-1}\big(1-\varphi i^{(0)}\big)^{-\frac{1}{\eta}-1}}{(\gamma-1)\eta} \times \\
&\big(\psi^{(1)}(E,H)(1-\eta)(1-\varphi i^{(0)}) + (\gamma-1)\varphi i^{(1)}\psi^{(0)}(E,H)\big),
\end{aligned}
$$

which can be solved for $i^{(1)}$ in terms of $\psi^{(1)}$, i.e.,

$$
i^{(1)} = \psi^{(1)}(E,H)\frac{\psi^{(0)}(E,H)^{\frac{1-\eta}{(\gamma-1)\eta}-1}\big(1-\varphi i^{(0)}\big)^{-\frac{1}{\eta}-1}(1-\eta)(1-\varphi i^{(0)})}{(\gamma-1)\big(\varphi\psi^{(0)}(E,H)^{\frac{1-\eta}{(\gamma-1)\eta}}\big(1-\varphi i^{(0)}\big)^{-\frac{1}{\eta}-1} + \eta\big)}. \tag{41}
$$

Substituting $i^{(1)}$ from (41) and the zeroth-order solution for ψ_0 from (38), we obtain after considerable but trivial manipulations that

$$
\epsilon\psi^{(1)}(E,H) = \frac{h(E,H)}{r^\star}\Big(\psi(E,H+1) - \psi^{(0)}(E,H)\Big), \tag{42}
$$

where $r^\star$ was obtained as part of the zeroth-order solution and is given by (18).

Proof of Result 2 Combining the zeroth- and first-order solutions (38) and (42) gives $J = J^{(0)} + \epsilon J^{(1)} = \psi K^{1-\gamma}/(1-\gamma)$ with ψ defined by

$$\psi(E,H) = \psi^{(0)}(E,H) + \frac{h(E,H)}{r^\star}\big(\psi(E,H+1) - \psi^{(0)}(E,H)\big),$$

where in the terminal state $\psi(E,\overline{H}) = \psi^{(0)}(E,\overline{H})$. The optimal SCC follows from evaluating $P = -\frac{J_E}{J_K} q = \frac{\psi_E(E,H)}{\psi(E,H)} \frac{qK}{\gamma-1}$ with

$$\psi_E(E,H) = \psi_E^{(0)}(E,H) + \frac{h(E,H)}{r^\star}\big(\psi_E(E,H+1) - \psi_E^{(0)}(E,H)\big) + \frac{\partial h(E,H)}{\partial E}\frac{1}{r^\star}\big(\psi(E,H+1) - \psi^{(0)}(E,H)\big). \tag{43}$$

Truncating the denominator of $\frac{\psi_E(E,H)}{\psi(E,H)}$ and Tobin's Q at zeroth order for consistency and using $P_{\text{R1}}(E,H) = \frac{\psi_E^{(0)}(E,H)}{\psi^{(0)}(E,H)} \frac{qK}{\gamma-1}$, we obtain equation (28). □

Appendix B: Derivation of the market-based calibration

Assuming no negative impact of climate change on the economy, we can derive closed-form expressions for our key economic variables. Given the parameter values for economic uncertainty and the share of fossil-fuel use, we calibrate the remaining parameters to match an expected GDP growth rate of $g^{(0)} = 2\%$ in normal times, i.e., in the absence of rare macroeconomic disasters, an average consumption rate of $\chi^{(0)} \equiv \frac{C^{(0)}}{B^{(0)}K} = 73\%$ of GDP, a risk-free interest rate of $r_f = 0.8\%$/year, an equity risk premium of $r_p = 6.5\%$/year, a return on risky assets of 7.3%/year, and a Tobin's Q of $q^{(0)} = 1.38$. The following five equations give a non-linear system that relates ρ, γ, $B^{(0)}$, δ, and φ to those quantities:

$$\chi^{(0)} = \frac{q^{(0)}}{B^{(0)}}\Big[\rho + (\eta-1)\Big(\overline{g}^{(0)} - 0.5\gamma\sigma^2 - \frac{\lambda_e}{\beta_e - \gamma + 1}\Big)\Big], \tag{44}$$

$$\overline{g}^{(0)} = -\delta + B^{(0)}\big(1 - \chi^{(0)} - \alpha\big) - \frac{1}{2}\varphi\big(B^{(0)}\big)^2\big(1 - \chi^{(0)} - \alpha\big)^2 - \frac{\lambda_e}{\beta_e + 1}, \tag{45}$$

$$r_f = \rho + \eta\overline{g}^{(0)} - \frac{1}{2}\gamma(1+\eta)\sigma_c^2 - \lambda_e\frac{(\eta-\gamma)(\alpha_e-\gamma) + \gamma(\beta_e - \gamma + 1)}{(\alpha_e - \gamma)(\alpha_e - \gamma + 1)}, \tag{46}$$

$$r_p = \gamma\sigma^2 + \lambda_e\gamma\Big[\frac{1}{\beta_e - \gamma} - \frac{\beta_e}{(\beta_e + 1)(\beta_e - \gamma + 1)}\Big], \tag{47}$$

$$q^{(0)} = \frac{1}{1 - \varphi i^{(0)}}. \tag{48}$$

See also Pindyck and Wang (2013) and Hambel et al. (2024).

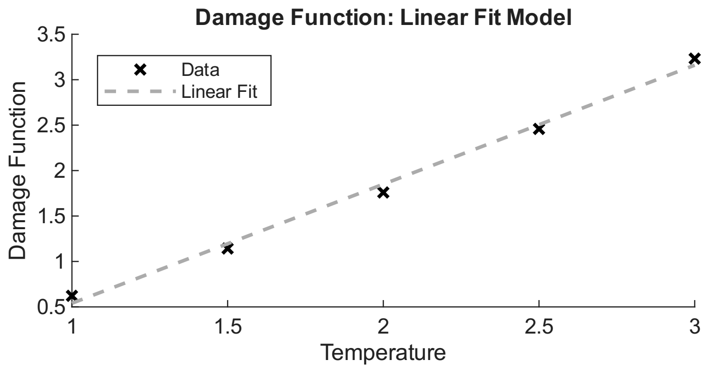

FIGURE C.1. Calibration of Climate Damages. The figure shows the damage function of Howard and Sterner (2025) in the range of 1°C to 3°C and the linear fit (grey dashed line).

APPENDIX C: CALIBRATION OF CLIMATE DAMAGES AND DISASTER RISK

TFP Damages We calibrate our climate damage function so it fits the non-catastrophic convex damage function $D = 0.00622T^{1.5}$ of Howard and Sterner (2025) in the range of 1°C to 3°C. Figure C.1 illustrates the non-catastrophic damage function of Howard and Sterner (2025) (black data) and the linear fit (see the dashed grey dashed line . The quality of the fit is very high ($R^2 = 99.42\%$). The linear damage function thus provides a reasonable approximation to a convex damage function in the range of up to 3°C.

Disaster Risk As described in Section 5.3, we base our calibration of temperature-related risk of climate disasters on Karydas and Xepapadeas (2022).[40] Panel (a) of Figure C.2 illustrates their data along with the fit of a linear function $\lambda(t) = \lambda_0 + \lambda_1 T$ to the data. The quality of the fit is high ($R^2 = 91.67\%$).

However, recent evidence suggests that temperature may increase the hazard rate of climate-related disasters exponentially rather than linearly (e.g., Davariashtiyani et al., 2023, Russo and Domeisen, 2023). Therefore, we have fitted two exponential functions to this data. The best exponential fit (see the dark dashed grey line in panel (b)) leads to an intensity function that is very similar to the linear function in the relevant range. The quality of this exponential fit is even slightly worse than that of the linear function ($R^2 = 91.28\%$), which further supports the use of a linear function. Finally, we fit an exponential function, while excluding the last data point (0.87 | 0.066). This gives the exponential disaster intensity $\lambda_c(T) = 1.26\mathrm{e}^{0.0845T} - 1.27$ and an even better fit ($R^2 = 96.62\%$). This function deviates slightly from the linear fit if we consider a higher temperature range of up to two degrees (see dashed grey dashed line in panel (b)).

Modified Rule To account for the non-linear effect of the disaster intensity, we replace λ_{1T} in Rule 1 by the marginal disaster intensity $\frac{\partial \lambda^c(T)}{\partial T}$. Rule 1 then becomes

$$P_t = \left[D_{1T} + \frac{\partial \lambda^c(T)}{\partial T} \frac{\mathbb{E}\left[1 - Z_c^{1-\gamma}\right]}{1-\gamma} \frac{q^{(0)}}{B^{(0)}} \right] \frac{\chi Y_t^{(0)}}{r^\star}.$$

[40]We thank the authors for sharing their data with us.

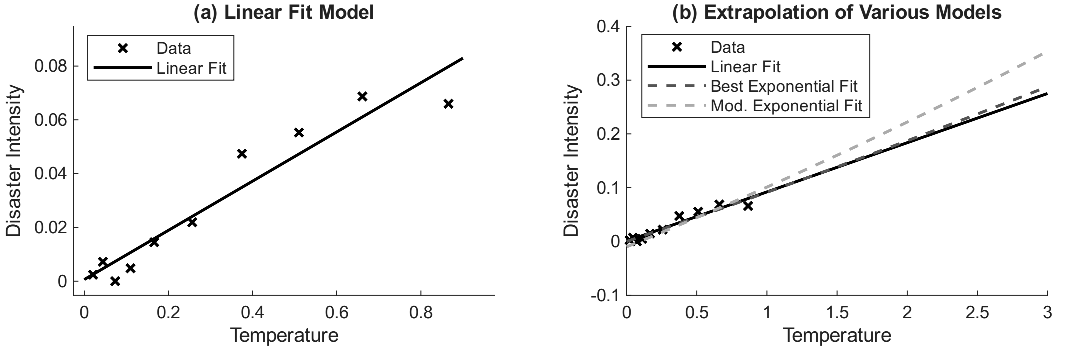

FIGURE C.2. Calibration of Climate-Related Disasters. The figure illustrates the historical relationship between global average temperature and the intensity of natural disasters. The data is taken from Karydas and Xepapadeas (2022). Panel (a) shows the data in the range between 0 and 0.9 degrees and illustrates the fit of a linear function $\lambda(t) = \lambda_0 + \lambda_1 T$ to the data. Panel (b) shows a temperature range of up to 2°C and compares the linear fit with two exponential fits.

For $\lambda^c(T) = \mathrm{e}^{\lambda_0+\lambda_1 T}$, we use $\frac{\partial \lambda^c(T)}{\partial T} = \lambda_1 \mathrm{e}^{\lambda_0+\lambda_1 T}$ in the expression for P_t. We use this new rule to evaluate the SCC with exponential disaster intensities and find that the rule has decent accuracy, although we only use the zeroth-order solution. The accuracy of this rule can be improved further if one uses a first-order solution even without tipping risk. This would give an additional convexity markup term (cf. Result 2 and online Appendix A.4.2 of van den Bremer and van der Ploeg (2021)).

APPENDIX D: FURTHER DETAILS ON CLIMATE RISK AND TIPPING POINTS

In Section 7, we consider two variants of our climate model.

Stochastic Climate Dynamics First, we equip the climate model (4) with normally-distributed shocks, i.e., we replace (4) by

$$T_t = \chi(H_t)E_t + \int_0^t \sigma_T(H_s)\mathrm{d}W_{Ts},$$

where W_{Tt} is a second Wiener process modelling temperature shocks and $\sigma_T(H_t) \geq 0$ the relative volatility of those temperature shocks. This makes temperature an additional state variable and leads to additional terms in the HJB equation.[41] We choose a constant temperature volatility of $\sigma_T = 0.033$ to match the temperature range of global mean temperature increase in the RCP scenarios.[42] Since the shocks are normally distributed, our simple rules for the optimal SCC are not affected.

[41] If we assume that the ratio $\sigma_T(H_t)/\chi(H_t)$ is constant for all states H and is denoted by σ_E, we can rewrite the model in the state variables H and E where the modified dynamics of E reads $\mathrm{d}E_t = \varpi F_t \mathrm{d}t + \sigma_E \mathrm{d}W_{Tt}$. This simplification has no significant effect on the optimal SCC, but it significantly simplifies and accelerates the numerical solution.

[42] The temperature range in the year 2100 of the various RCP scenarios varies between 0.8°C around its mean in RCP2.6 to 1.1°C in RCP8.5.

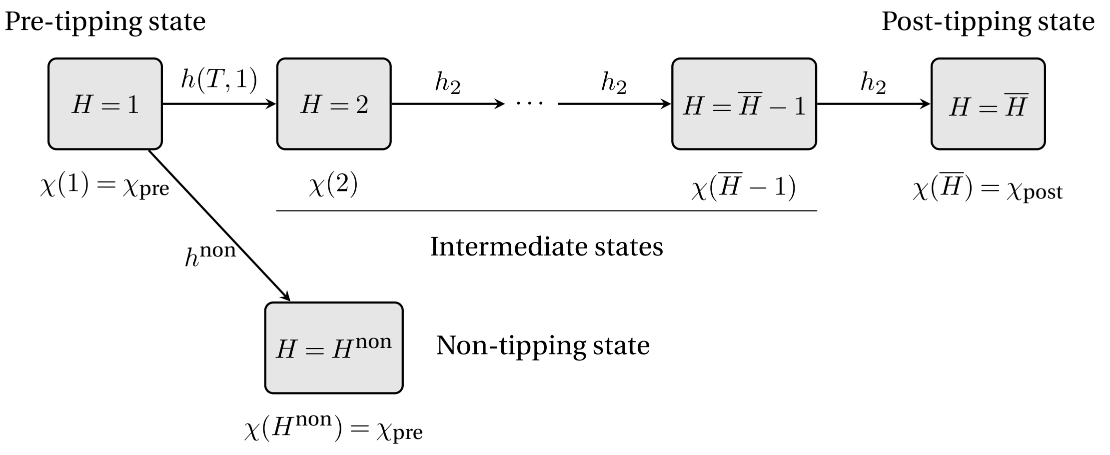

FIGURE D.1. Structure of the Gradual Climate Tipping Process with Non-tipping state. The figure illustrates how climate tipping propagates from a pre-tipping state $H = 1$ through several intermediate states to a post-tipping state $H = \overline{H}$ with $\chi_{\text{post}} > \chi_{\text{pre}}$ and how this gradually increases the TCRE. It also illustrates the possibility that tipping never happens when transitioning to the non-tipping state $H = H^{\text{non}}$.

More Sophisticated Climate Tipping To account for the probability that tipping never happens, we model an additional absorbing state in which the TCRE remains unchanged from its initial state. This extra state is denoted by H^{non} and referred to as a non-tipping state. The transition intensity from the pre-tipping state to the non-tipping state is denoted by h^{non}. Once the Markov chain transitions to this state, one learns that tipping never happens. In our numerical implementation, we use $h^{\text{non}} = 0.35\%$/year.

Figure D.1 depicts the structure of this Markov chain. This additional state requires repricing in the pre-tipping state. Since $\psi(E, H^{\text{non}}) = \psi^{(0)}(E, 1)$, the modified rule for the optimal SCC in the pre-tipping state $H = 1$ is

$$P = P_{\text{R2}} + h^{\text{non}} \frac{1}{r^\star} (P_{\text{R1}} - P_{\text{R2}}) . \tag{49}$$

Starting with the optimal carbon price from Rule 2, we now have to take another correction term into account, because we can jump to the non-tipping state with intensity h^{non}. Similarly, further absorbing states can be included in the Markov chain, so that it is not known in advance at which new TCRE the cascade will end. This would generally result in further correction terms. Overall, these absorbing states reduce the SCC in the pre-tipping state.

APPENDIX E: ADDITIONAL ACCURACY CHECKS

Small parameter assumptions Our perturbation analysis gives an accurate estimate of the optimal SCC if our small parameters are 'small'. To test whether the small parameters are indeed small enough, we examine how the accuracy of the rule varies with the size of the small parameters.

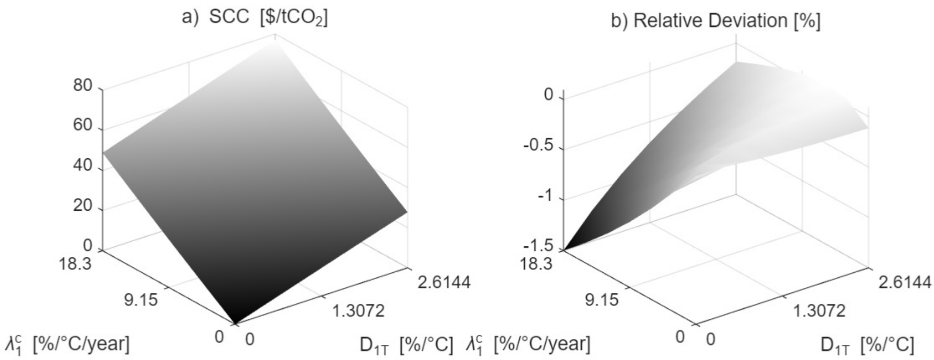

FIGURE E.1. Sensitivity of the SCC and Accuracy without Climate Tipping Risk ($h = 0$). Panel (a) illustrates how the marginal effect of temperature on the damage ratio D_{1T} and the marginal effect of temperature on the intensity of climate-related macroeconomic disasters λ_1^c affect the optimal SCC if temperature is fixed at $T_0 = 1.1°$C. Note that the benchmark calibration values are $D_{1T} = 1.31\%/°$C and $\lambda_1^c = 0.0006 + 9.15 \times 1.1 = 9.15\%$/year. Panel (b) illustrates the relative deviation between the rule and the numerical optimum as a function of these parameters.

Figure E.1 does this for the first two small parameters, i.e., the marginal effect of temperature on the damage ratio D_{1T} and the marginal effect of temperature on the intensity of climate-related macroeconomic disasters λ_{1T}^c, by showing how the optimal SCC, both evaluated with our simple rule and with numerical optimisation, varies with these two parameters (without risk of a climate tipping point, $h(E, H) = 0$). The left-hand panel confirms that a higher adverse effect of temperature on total factor productivity D_{1T} and on the risk of recurring disasters λ_{1T}^c increases the SCC, according to our rule. The right-hand panel shows that the relative approximation error compared with full numerical optimisation varies from $+0.3\%$ to -1.5%. The rule thus performs well for a realistic range of the size of the first two small parameters with the market-based calibration. The relative error of the two individual components is small. While the relative error of the TFP component is always close to zero, the biggest approximation error is made when disaster risk is twice as pronounced as in the benchmark calibration. In this case, the error of this component is -1.5%. For the ethics-based calibrations, the relative error of the disaster component becomes a bit more pronounced, reaching up to -3.3% when disaster risk is twice as pronounced as in the benchmark calibration with $r^* = 3\%$.[43]

We also consider the accuracy of our rule when there is a risk of gradual climate tipping. Figure E.2 is the same as Figure E.1 but with $h_{1T} = 0.35\%/°$C/year. We confirm again that the optimal SCC is higher, the more sensitive the adverse effects of global warming on total factor productivity and on the risk of recurring climate-related disasters are to temperature (D_{1T} and λ_{1T}^c, respectively). Relative approximation errors remain small, ranging from –0.6% to 1.5% of the optimal SCC.

[43]These results are available upon request.

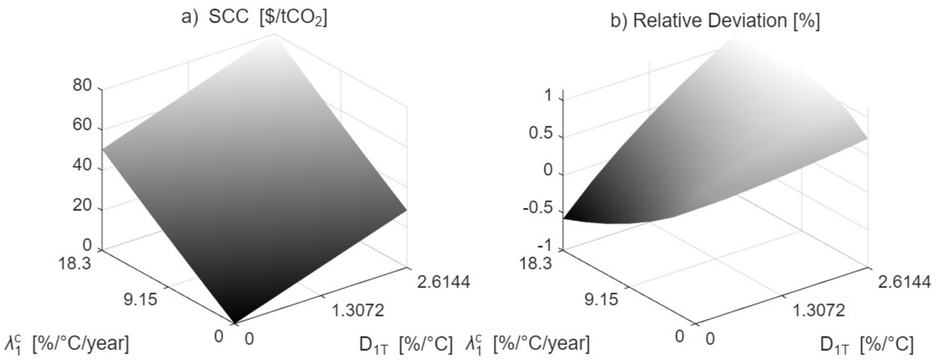

FIGURE E.2. Sensitivity of the SCC and Accuracy with Climate Tipping Risk ($h_{1T} = 0.6\%$/°C/year). Panel (a) illustrates how the marginal effect of temperature on the damage ratio D_{1T} and the marginal effect of temperature on the intensity of climate-related macroeconomic disasters λ^c_{1T} affect the optimal SCC (for $T_0 = 1.1°$C). Panel (b) illustrates the relative deviation between the simple rule and the numerical optimum as a function of the same parameters.

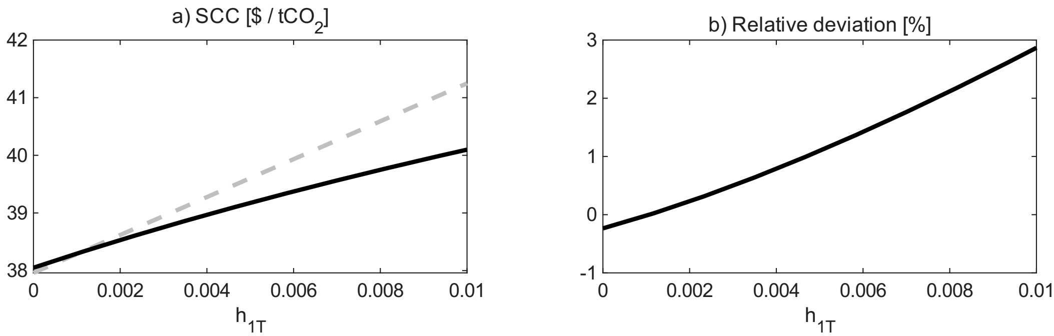

FIGURE E.3. Tipping Risk Sensitivity of the Optimal SCC with $r^\star = 5.3\%$/year ($D_{1T} = 1.31\%/°$C, $\lambda^c_{1T} = 9.15\%/°$C/year). Panel (a) illustrates how the marginal effect of temperature on the intensity of climate tipping h_{1T} affects the optimal social cost of carbon (for $T_0 = 1.1°$C). The benchmark value is $h_{1T} = 0.35\%/°$C/year. The black line show the numerical solution and the grey dashed line the SCC determined by Result 2. Panel (b) shows the relative deviation between the simple rule and the numerical optimum as a function of the parameter h_{1T}.

Now we test the accuracy of our rule with respect to the hazard rate of climate tipping $h = h(E, H)$. To do so, we vary the marginal effect of temperature on this hazard rate, h_{1T}. In doing so, we vary the size of two small parameters simultaneously ($\hat{h}_{0,\text{pre}}$ and $\hat{h}_1$). Figure E.3, panel (a) shows how varying the size of this parameter impacts the optimal SCC. For this purpose, we consider the benchmark model with all three externalities and vary h_{1T} in the range $[0, 1]$ %/year/°C.[44] The figure shows that a higher in-

[44]A marginal hazard rate of 1%/year/°C is far outside the consensus range. For instance, Cai and Lontzek (2019) perform sensitivity analyses with marginal hazard rate of 0.25%/year/°C and 0.45%/year/°C. Never-

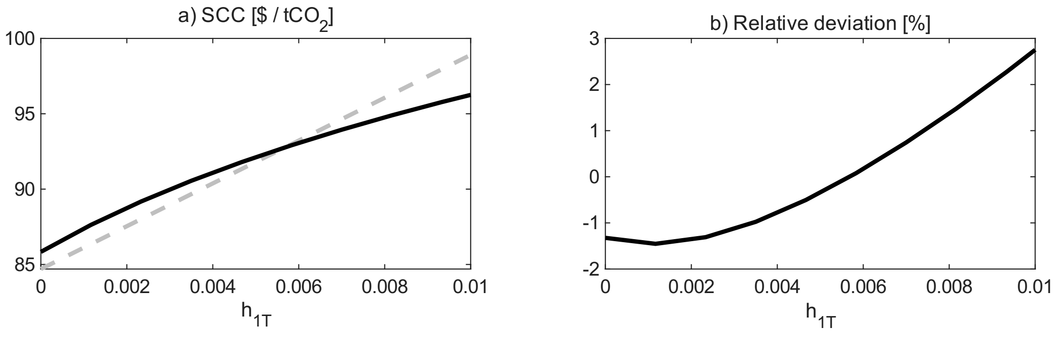

FIGURE E.4. Tipping Risk Sensitivity of the Optimal SCC with $r^\star = 3\%$/year ($D_{1T} = 1.31\%/^\circ$C, $\lambda^c_{1T} = 9.15\%/^\circ$C/year). Panel (a) illustrates how the marginal effect of temperature on the intensity of climate tipping h_{1T} affects the optimal social cost of carbon (for $T_0 = 1.1^\circ$C). The benchmark value is $h_{1T} = 0.35\%/^\circ$C/year. The black line show the numerical solution and the grey dashed line the SCC determined by Result 2. Panel (b) shows the relative deviation between the simple rule and the numerical optimum as a function of the parameter h_{1T}.

tensity of climate tipping points increases the SCC almost linearly according to our rule as shown by the grey dashed line , where the convex error reflects the validity of our estimate for the SCC up first order in the small parameter, resulting in second-order errors. The figure also suggests that the true SCC obtained numerically reacts in a more concave manner to the tipping probability, even if this probability is linear in temperature. Panel (b) shows that the relative error compared with numerical optimisation varies from less than 0.04% if tipping is switched off to about 3% if the marginal hazard rate h_{1T} is 1% (almost three times that in the benchmark calibration). The rule for the optimal SCC thus performs very well.

We also analyse the relative approximation error of the tipping component in greater detail. As discussed in Section 6.1, this error can be sizeable in relative terms (up to 60% in some extreme parametrisations with 40% in the benchmark calibration), but it remains small in absolute terms. In all of our numerical experiments, it is below one dollar and thus economically not significant. For lower discount rates, the relative error of the tipping component becomes much smaller (below 10% in most cases and only 3% in the benchmark calibration), which is tolerable as tipping contributes significantly less to SCC than climate-related disaster risk. Figure E.4 shows the counterpart of Figure E.3 for a discount rate of $r^\star = 3\%$, showing that the bigger errors for large hazard rates do not grow further if we use a lower discount rate.

Growth- and risk-adjusted discount rate A key parameter in our simple rule is the growth and risk-adjusted discount rate r^*. We calibrate the model with a rate of $r^* = 5.3\%$ (3% and 2% for the ethics-based calibrations) in the absence of climate impacts. Taking climate impacts into account slightly reduces those rates. To further test the accuracy of our rule, we compare the growth- and risk-adjusted discount rate used to cal-

theless, precisely because there is a high degree of uncertainty regarding this parameter and the calibration is somewhat speculative, we are testing our rule for a significantly larger range.

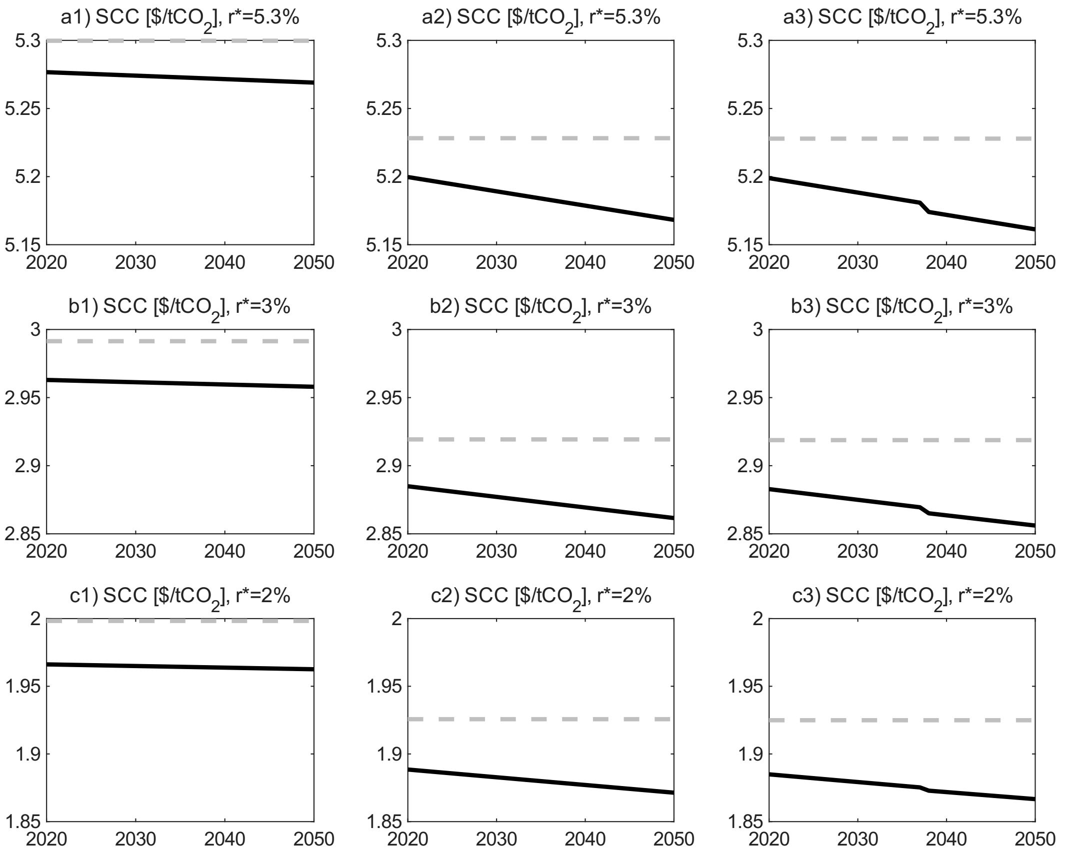

FIGURE E.5. Simulation of the growth and risk adjusted discount rate. Column a) refers to the market-based calibration. Columns b) and c) refer to the ethics-based choices of utility discount rates. Row 1 considers the case with TFP damages only, row 2 considers TFP damages and recurring climate disasters, and row 3 considers all three externalities with climate tipping happening in the year 2038. The black lines depict the time path of $r^{\star}$ determined numerically, and the grey dashed lines give $r^{\star}$ determined analytically and used for our rules.

culate the SCC in the simple rule with its numerically calculated counterpart. Figure E.5 illustrates this comparison for nine scenarios. Column a) refers to the market-based calibration. Columns b) and c) refer to the ethics-based choices of utility discount rates. Row 1 considers the case with TFP damages only, row 2 considers TFP damages and recurring climate disasters, and row 3 considers all three externalities. The black lines depict the time path of $r^{\star}$ determined numerically, and the grey dashed lines give $r^{\star}$ determined analytically from our rule for the optimal SCC.

Overall, the accuracy is high, and the starting value of r^{*} in (23) and (24) is close to its numerical optimum. The differences are economically not significant and amount to 2 basis points for the market-based calibrations and about 3.5 basis points for the ethics-based calibrations. While the rules use a constant discount rate, the numerical solution takes into account the progression of climate change and the change in the discount rate along the time path. Thus, the differences become a bit more pronounced along the time path when climate change propagates, but will remain at a maximum of 5 basis points until 2050. Notice that in column 3, climate tipping happens in the year 2038, which leads to a slight shock to the discount rate of about one additional basis point. Overall, those results indicate high accuracy of our approximated discount rates (23) and (24).

Appendix F: Numerical solution approach

In order to solve the model numerically, we first decompose the value function into two parts and reduce the number of state variables by one. This leads to a simplified HJB equation, which can then be solved numerically more easily.

F.1 *Auxiliary calculations*

Aggregate consumption is given by

$$C \equiv A\big[1 - D(E,H)\big]K^{\alpha}F^{1-\alpha} - I - bF.$$

The HJB equation for the general case with three global warming externalities is

$$\max_{C,F}\Big[f\big(C,J\big) + J_K\Big[A(E,H)K^{\alpha}F^{1-\alpha} - C - bF - \delta K - \frac{1}{2}\varphi\frac{I^2}{K}\Big] + \frac{1}{2}J_{KK}K^2\sigma^2 + J_E\varpi F$$
$$+ \lambda_e\mathbb{E}\big[J\big((1-\ell_e)K,E,H\big) - J(K,E,H)\big] + \lambda_c(E,H)\mathbb{E}\big[J\big((1-\ell_c)K,E,H\big) - J(K,E,H)\big]$$
$$+ h(E,H)\big[J(K,E,H+1) - J(K,E,H)\big]\Big] = 0.$$

Define $f = F/K$, $i = I/K$, and $c = C/K$. Conjecture a value function of the form

$$J(K,E,H) = \frac{1}{1-\gamma}K^{1-\gamma}V(E,H).$$

The Epstein–Zin aggregator is then given by

$$\frac{1}{1-\eta}\frac{C^{1-\eta} - \rho[(1-\gamma)J]^{\frac{1-\eta}{1-\gamma}}}{[(1-\gamma)J]^{\frac{1-\eta}{1-\gamma}-1}} = \rho\theta c^{1-\eta}V^{1-1/\theta}u(K) - \rho\theta u(K)V,$$

where $u(K) \equiv \frac{1}{1-\gamma}K^{1-\gamma}$ and $\theta \equiv \frac{1-\gamma}{1-\eta}$. Substituting the conjecture and its partial derivatives into the HJB equation and dividing by $u(K)$ yields the HJB equation for $V = V(E,H)$,

$$\begin{aligned} 0 = \max_{F,I}\Big[&\rho\theta V^{1-1/\theta}c^{1-\eta} - \rho\theta V + V(1-\gamma)\big(-\delta + i - \tfrac{1}{2}\varphi i^2\big) + V_E f K_0 - \tfrac{1}{2}\gamma(1-\gamma)\sigma^2 V \\ &+ V\lambda_e\mathbb{E}[(1-\ell_e)^{1-\gamma} - 1] + V\lambda_c(E,H)\mathbb{E}[(1-\ell_c)^{1-\gamma} - 1] \\ &+ h(E,H)\big[V(E,H+1) - V(E,H)\big]\Big], \end{aligned} \tag{50}$$

where $c = A(E,H)f^{1-\alpha} - i - bf$.

F.2 *Numerical algorithm*

Basic idea We face a time-homogeneous problem with an infinite time horizon. We transform this HJB equation into a parabolic PDE by adding a time derivative to the HJB equation. Starting from the terminal condition, we move backwards through the time grid until the difference in the value function between time t and $t+1$ becomes negligibly small. Since the boundary conditions on V are unknown, we transform the problem into a similar one with a finite time horizon denoted by $t_{\max}$. In our implementation, we consider a model with a finite time horizon and choose a conjecture for $V(t_{\max}, E, H)$, which mimics the shape of the true yet unknown value function.[45] Starting with this terminal condition, we work backwards through the time grid until the differences between the value function in $t+1$ and t become negligibly small and the solution converges to that of an infinite time horizon.

Definition of the grid We use a grid-based solution approach to solve the non-linear PDE. We discretise the (t, E)-space using an equally-spaced lattice. Its grid points are defined by

$$\left\{(t_n, E_i) \mid n = 0, \cdots, N_t, \, i = 0, \cdots, N_E\right\},$$

where $t_n = n\Delta_t$ and $E_i = i\Delta_E$ for some fixed grid size parameters Δ_t and Δ_E that denote the distances between two grid points. The numerical results are based on a choice of $N_E = 100$ and 1 time step per year. Our results hardly change if we use a finer grid or more time steps per year. In the sequel, $V_{n,i,j}$ denotes the approximated value function at the grid point (t_n, E_i, H_j) and $\pi_{n,i,j}$ refers to the corresponding set of optimal controls. We apply an implicit finite-difference scheme.

Finite-differences approach We now describe the numerical solution approach in more detail. We adapt the numerical solution approach used by Munk and Sørensen (2010). The numerical procedure works as follows. At any point in time, we make a conjecture for the optimal strategy $\pi^*_{n,i,j}$. A good guess is the value at the previous grid point since the abatement strategy varies only slightly over a small time interval, i.e., we set $\pi_{n-1,i,j} = \pi^*_{n,i,j}$. Substituting this guess into the HJB equation yields the semi-linear PDE[46]

$$0 = \rho\theta V^{1-1/\theta} c^{1-\eta} + M_1 V + M_2 V_E + M_3 V(t, E, H+1) \tag{51}$$

[45]We have tested several conjectures and find that the concrete choice of $V(t_{\max}, E, H)$ only affects how long it takes until the algorithm converges, but does not affect the limit itself. An obvious conjecture is the leading-order approximation for the value function, i.e., $V = \psi$.

[46]Our benchmark problem has only one continuous state variable E. It is straightforward to extend the algorithm to the case with two continuous state variables, which is necessary, for instance, in the two-sector model discussed in Section 7, where the share of brown capital is another continuous state variable. For technical details, we refer to Appendix B of Hambel et al. (2024). Similarly, in Section 7, we have an additional second-order derivative when there are stochastic dynamics in the temperature dynamics and an additional jump component when there is the possibility of tipping never occurring.

with state-dependent coefficients $M_k = M_k(t,E,H)$, see equation (50). Notice that in the absorbing post-tipping state, $M_3(t,E,\overline{H}) = 0$. Due to the implicit approach, we approximate the time derivative by forward finite differences. In the approximation, we use the so-called 'up-wind' scheme that stabilises the finite-difference approach. Therefore, the relevant finite differences at the grid point (n,i,j) are given by

$$\mathrm{D}_E^+ V_{n,i,j} = \frac{V_{n,i+1,j} - V_{n,i,j}}{\Delta_E}, \quad \mathrm{D}_E^- V_{n,i,j} = \frac{V_{n,i,j} - V_{n,i-1,j}}{\Delta_E}, \quad \mathrm{D}_t^+ V_{n,i,j} = \frac{V_{n+1,i,j} - V_{n,i,j}}{\Delta_t}.$$

Substituting these expressions into the PDE above yields the following semi-linear equation for the grid point (t_n, E_i, H_j)

$$\begin{aligned} V_{n+1,i,j}\frac{1}{\Delta_t} = V_{n,i,j}\Big[-M_1 + \frac{1}{\Delta_t} + \mathrm{abs}\Big(\frac{M_2}{\Delta_E}\Big)\Big] + V_{n,i-1,j}\frac{M_2^-}{\Delta_E} - V_{n,i+1,j}\frac{M_2^+}{\Delta_E} \\ + \delta\theta V_{n,i,j}^{1-1/\theta} c_{n,i,j}^{1-1/\psi} - M_3 V_{n,i,j+1}. \end{aligned} \tag{52}$$

Therefore, for a fixed point in time, each grid point is determined by a nonlinear equation. Starting with the absorbing state $H_j = \overline{H}$, we can solve for the vector $V_{n,\overline{H}} \equiv (V_{n,1,\overline{H}}, \cdots, V_{n,N_E,\overline{H}})$ and substitute this result into (52). We subsequently move backwards through the Markov chain and determine $V_{n,j} \equiv (V_{n,1,j}, \cdots, V_{n,N_E,j})$ in each climate tipping state H_j. Using this solution, we update our conjecture for the optimal controls at the current point in the time dimension. We apply the above-mentioned first-order conditions and finite-difference approximations of the corresponding derivatives. Finally, we calculate the optimal SCC using those partial derivatives.

APPENDIX G: SLUGGISH RECOVERY OF THE CAPITAL STOCK

A neoclassical growth model with a Cobb-Douglas production function instead of an AK production function allows for *sluggish recovery* from a hit to the capital stock. One would thus expect that it is optimal to implement a lower carbon price than with an AK production structure. Alternatively, we expect our rule derived for a climate-economy model with AK growth to *overestimate the optimal SCC*, especially for the component of the SCC that has to correct for recurring climate disasters. To illustrate this, we apply our simple rule for the SCC to a neoclassical growth and climate model without AK growth. To keep matters simple, we do this numerically for a simple Solow-Swan version of our model with exogenous labour supply, exogenous TFP growth, climate disaster risk, and climate tipping risk. In this model, there are no adjustment costs and thus Tobin's Q is unity, and this simplifies our rule for the SCC somewhat.

Following the DICE-2023 model (Barrage and Nordhaus, 2024), gross output is

$$Y_t = A(t)K_t^{\alpha}L(t)^{1-\alpha}D(T_t) = I_t + C_t + Y_t\big[1 - a(t)\mu_t^b\big],$$

and emissions are given by $Y_t\sigma(t)[1-\mu_t]$, where μ_t denotes the emission control rate. Total factor productivity $A(t)$, labour $L(t)$, the abatement cost parameter $a(t)$, and the

TABLE G.1. Application of the Rule for the Optimal SCC (US $/t$CO_2$) developed for an AK economy to a Solow-Swan Model.

Market-based calibration with $r^\star = 5.3\%$/year

Externalities	Rule ($/t$CO_2$)	Share of SCC	Numerical ($/t$CO_2$)	Share of SCC	Relative Error
TFP damages only	13.92	43.0%	15.82	49.2%	–12.01%
+ climate disasters	17.36	53.6%	12.20	38.0%	42.30%
+ climate tipping	1.12	3.5%	4.11	12.8%	–72.75%
Total	32.40	100.0%	32.13	100.0%	0.84%

Note: The rule is applied outside the realm for which it was derived, i.e., in an exogenous growth model of the Solow-Swan type. The approximation errors in row "Total" are the weighted averages of the approximation errors of the three individual components. The components of the rule for the optimal SCC perform badly, especially for climate-related disasters and climate tipping points.

.

emission intensity $\sigma(t)$ evolve exogenously as specified in Barrage and Nordhaus (2024). Therefore, cumulative emissions follow the dynamics

$$\mathrm{d}E_t = Y_t\sigma(t)\left[1-\mu_t\right]\mathrm{d}t.$$

We calibrate the capital shocks so that the effect of Brownian shocks and disaster shocks on output is identical to that in the main model. An application of Itô's lemma shows that we must multiply the capital volatility from the benchmark calibration by the factor $1/\alpha$ and the curvature parameters of the disaster sizes by the factor α to obtain the same effects as in the main model.

Discussion Table shows how well our rule for an AK growth model (adjusted to allow for a Tobin's Q of 1) performs for the market-based calibration. The answer is coincidentally quite well for the total SCC, but badly for the individual components of the SCC. The SCC if only TFP damages are being internalised is out by about $2/t$CO_2$ or 12%. Interestingly, if in addition the temperature-dependent risks of recurring climate disasters are internalised, our rule for the optimal SCC gives (despite the under-estimate of the component due to TFP damages) an overestimate of the SCC. Our rule gives a figure for the SCC that is 42% higher than it should be. The reason is that our rule fails to account for capital shock recovery in the Solow-Swan model after a disaster.

To see this, note that the speed of adjustment for a Solow-Swan equals the product of $1-\alpha$ and the exogenous trend growth rate. Hence, there is no adjustment or recovery at all in the endogenous AK growth model with $\alpha = 1$. But with $0 < \alpha < 1$, the speed of adjustment or recovery rate is strictly positive. This is not captured by the disaster component of our rule for the SCC, so the rule overestimates the optimal SCC. The climate-tipping component of the rule for the optimal SCC also performs badly.

In fact, the first component of our simple rule related to productivity damages (i.e., $\chi D_{1T}Y/r^\star$) works reasonably well *provided* that the economy is close to or at the steady state. If we switch on disaster risk (which needs to be calibrated carefully) or climate tipping risk, the accuracy of the rule drops. And the further one moves away from the steady state, the less accurate the rule becomes. There are several other reasons other than sluggish recovery of the capital stock for this.

First, in an AK model, growth rates, the consumption-output ratio, interest rates, risk premiums, etc. are constant (if we ignore climate change), whereas in a neoclassical model they are state-dependent (through the capital stock) and time-dependent (through exogenous growth). Hence, the discount rate $r^\star$ is not constant anymore, which makes pricing more involved. This effect is particularly pronounced if the economy is hit by a big disaster shock that drives the economy far away from the steady state. If we only consider TFP damages and Brownian shocks, the state-dependency of $r^\star$ is less dramatic, leading to a quite accurate performance of the rule provided one is close to the steady state.

Second, the disaster component contains the risk-adjusted loss term $\mathbb{E}[1-Z^{1-\gamma}]/(1-\gamma)$, which translates shocks to the capital stock into utility units. In our AK model, the value function satisfies $J(K,E,H)=\frac{1}{1-\gamma}K^{1-\gamma}\psi(E,H)$ and optimal consumption can be expressed as $C=c(E,H)K$. In the neoclassical model, there is no such decomposition of the value function and consumption. Thus, how climate-related disasters are translated into utility losses is more involved. This is also why our rule for climate tipping performs poorly in the neoclassical model, even without climate-related disaster risk. These effects are particularly pronounced if the discount rate is small, since then future shocks that drive one away from the steady state will also be particularly significant.

APPENDIX H: DETAILED RESULTS FOR EXTENSIONS IN SECTION 7

Tables and give two extensions: (1) falling cost of green energy to fall; and (2) a green and a brown sector. Table shows results for an exponential disaster intensity, Table for stochastic climate dynamics, and Table for a modified climate tipping model. We show results for $r^\star=5.3\%$ and 2% with results for 3% in between those cases.

TABLE H.1. Road-Testing the Rule for the Optimal SCC (US $/t$CO_2$) with Technical Progress in Fossil Fuel Production.

(a) Market-based calibration with $r^\star = 5.3\%$/year

Externalities	Rule ($/t$CO_2$)	Share of SCC	Numerical ($/t$CO_2$)	Share of SCC	Relative Error
TFP damages only	13.92	35.6%	13.86	35.8%	0.43%
+ climate disasters	24.04	61.5%	23.88	61.7%	0.67%
+ climate tipping	1.15	2.9%	0.96	2.5%	19.79%
Total	39.11	100.0%	38.70	100.0%	1.06%

(b) Ethics-based calibration with $r^\star = 2\%$/year

Externalities	Rule ($/t$CO_2$)	Share of SCC	Numerical ($/t$CO_2$)	Share of SCC	Relative Error
TFP damages only	36.93	22.0%	35.8	20.3%	3.16%
+ climate disasters	116.3	69.2%	122.69	69.6%	–5.21%
+ climate tipping	14.94	8.9%	17.89	10.1%	–16.49%
Total	168.17	100.0%	176.38	100.0%	–4.65%

Note: The rule is tested outside the realm for which it was derived, namely when there is steady technical progress in fossil fuel extraction instead of a constant cost of fossil fuel. The approximation errors in row "Total" are the weighted averages of the approximation errors of the three individual components.

TABLE H.2. Road-testing the Optimal SCC (US $/t$CO_2$) in a Two-Sector Model of the Economy.

(a) Market-based calibration with $r^\star = 5.3\%$/year

Externalities	Rule ($/t$CO_2$)	Share of SCC	Numerical ($/t$CO_2$)	Share of SCC	Relative Error
TFP damages only	13.92	35.6%	13.90	35.2%	0.14%
+ climate disasters	24.04	61.5%	23.92	60.6%	0.50%
+ climate tipping	1.15	2.9%	1.63	4.1%	–29.45%
Total	39.11	100.0%	39.45	100.0%	–0.86%

(b) Ethics-based calibration with $r^\star = 2\%$/year

Externalities	Rule ($/t$CO_2$)	Share of SCC	Numerical ($/t$CO_2$)	Share of SCC	Relative Error
TFP damages only	36.93	22.0%	36.30	22.9%	1.74%
+ climate disasters	116.3	69.2%	108.69	68.7%	7.00%
+ climate tipping	14.94	8.9%	13.18	8.3%	13.35%
Total	168.17	100.0%	158.17	100.0%	6.32%

Note: The rule is tested outside the realm for which it was derived, namely when there is a carbon-intensive and a green sector instead of one sector of the economy. The approximation errors in row "Total" are the weighted averages of the approximation errors of the three individual components.

TABLE H.3. Calculation of the Optimal SCC (US \$/tCO_2) with Exponential Climate Disasters.

(a) Market-based calibration with $r^\star = 5.3\%$/year

Externalities	Rule (\$/tCO_2)	Share of SCC	Numerical (\$/tCO_2)	Share of SCC	Relative Error
TFP damages only	13.92	30.1%	13.94	29.9%	–0.14%
+ climate disasters	30.90	66.8%	31.7	67.9%	–2.52%
+ climate tipping	1.41	3.0%	1.03	2.2%	36.89%
Total	46.23	100.0%	46.67	100.0%	–0.94%

(b) Ethics-based calibration with $r^\star = 2\%$/year

Externalities	Rule (\$/tCO_2)	Share of SCC	Numerical (\$/tCO_2)	Share of SCC	Relative Error
TFP damages only	36.93	17.8%	37.25	17.0%	–0.86%
+ climate disasters	150.61	72.6%	160.88	73.6%	–6.38%
+ climate tipping	20.05	9.7%	20.60	9.4%	–2.67%
Total	207.59	100.0%	218.73	100.0%	–5.09%

Note: The table summarises the results for the rule with exponential disaster intensity and compares the performance of that rule to the numerically optimised value of the SCC. The approximation errors in row "Total" are the weighted averages of the approximation errors of the three individual components.

TABLE H.4. Calculation of the Optimal SCC (US \$/tCO_2) with Stochastic Temperature Shocks.

(a) Market-based calibration with $r^\star = 5.3\%$/year

Externalities	Rule (\$/tCO_2)	Share of SCC	Numerical (\$/tCO_2)	Share of SCC	Relative Error
TFP damages only	13.92	35.6	13.94	35.9	–0.14%
+ climate disasters	24.04	61.5	24.12	62.1	–0.33%
+ climate tipping	1.15	2.9	0.80	2.1	43.75%
Total	39.11	100.0%	38.86	100.0%	0.64%

(b) Ethics-based calibration with $r^\star = 2\%$/year

Externalities	Rule (\$/tCO_2)	Share of SCC	Numerical (\$/tCO_2)	Share of SCC	Relative Error
TFP damages only	36.93	22.0%	37.25	21.6%	–0.86%
+ climate disasters	116.3	69.2%	120.3	69.6%	–3.33%
+ climate tipping	14.94	8.9%	15.2	8.8%	–1.71%
Total	168.17	100.0%	172.75	100.0%	–2.65%

Note: The table summarises the results for the rule and compares the performance of that rule to the numerically optimised value of the SCC when the climate system is exposed to normally-distributed temperature shocks. The approximation errors in row "Total" are the weighted averages of the approximation errors of the three individual components.

TABLE H.5. Calculation of the Optimal SCC (US $/t$CO_2$) with a Non-tipping state.

(a) Market-based calibration with $r^\star = 5.3\%$/year

Externalities	Rule ($/t$CO_2$)	Share of SCC	Numerical ($/t$CO_2$)	Share of SCC	Relative Error
TFP damages only	13.92	35.7%	13.94	35.9%	–0.14%
+ climate disasters	24.04	61.6%	24.11	62.1%	–0.29%
+ climate tipping	1.07	2.7%	0.75	1.9%	42.67%
Total	39.03	100.0%	38.8	100.0%	0.59%

(b) Ethics-based calibration with $r^\star = 2\%$/year

Externalities	Rule ($/t$CO_2$)	Share of SCC	Numerical ($/t$CO_2$)	Share of SCC	Relative Error
TFP damages only	36.93	22.3%	37.25	21.9%	–0.86%
+ climate disasters	116.36	70.3%	119.96	70.5%	–3.00%
+ climate tipping	12.17	7.4%	12.98	7.6%	–6.24%
Total	165.46	100.0%	170.19	100.0%	–2.78%

Note: The table summarises the results for the rule and compares the performance of that rule to the numerically optimised value of the SCC when there is a chance that tipping risk can disappear. The approximation errors in row "Total" are the weighted averages of the approximation errors of the three individual components.

Co-editor [Name Surname; will be inserted later] handled this manuscript.